Late Glacial and Holocene avulsions of the Rio Pastaza Megafan (Ecuador- Peru): frequency and controlling factors

Carolina Bernal, Frédéric Christophoul, José Darrozes, Jean-Claude Soula, Patrice Baby, José Burgos

Late Glacial and Holocene avulsions of the Rio Pastaza Megafan (Ecuador-Peru): Frequency and controlling factors

Carolina Bernal, Frédéric Christophoul, José Darrozes, jean-Claude Soula, Patrice Baby, José Burgos.

International Journal of Earth Sciences (2011), 100, 1759-1782
DOI 10.1007/s00531-010-0555-9
hal-00536576

C. Bernal, F. Christophoul, J-C. Soula, J. Darrozes and P. Baby, UMR 5563 GET, Université de Toulouse-CNRS-IRD-OMP-CNES,14 Avenue Edouard Belin, 31400 Toulouse, France. frederic.christophoul@get.obs-mip.fr

C. Bernal, chavelacarola@yahoo.com.mx
J-C. Soula, soula@get.obs-mip.fr
J. Darrozes, darrozes@get.obs-mip.fr
Patrice Baby, patrice.baby@ird.fr

J. Burgos,
Petroamazonas, Av. Naciones Unidas E7-95 y Shyris, Quito, Ecuador, 4to piso, Quito, Ecuador
jose_burgos@petroamazonas.ec

ABSTRACT The geomorphological study by mean of remote sensing imagery of the Rio Pastaza Megafan (Ecuador and northern Peru), reveals the traces of numerous avulsions. 108 avulsion sites have been defined. The location of these sites, the available radiocarbon ages as well as historical maps of the 17th century, enable us to propose an evolution history of the migration and avulsions of the Rio Pastaza since the Last Glacial Maximum. The first avulsions of the Río Pastaza occurred after the LGM in a zone close to and roughly parallel to the sudandean front, where the developed avulsion gave a distributive pattern to the ancient stream of the Río Pastaza in an area located between the modern Río Morona and Pastaza, where they caused the Rio Pastaza to develop a fan-like distributary pattern. This is interpreted as a response to thrust related forelimb tilt, progressively shifting eastward the Rio Pastaza and the apex of the megafan. This sequence of events ended with the Great Diversion of the Rio Pastaza toward the modern Rios Corrientes and Tigre. Avulsions occurred in the Tigre-Corrientes Area between 9200 and 8500 yrsCal BP. Afterward, the Río Pastaza was diverted to its present-day north-south course. This last significant avulsion occurred before AD 1691. In the area located between the modern Río Morona and Pastaza, avulsion frequency - probably overestimated - ranges between 100 to 200yrs. In the Ríos Tigre and Corrientes area, avulsion frequency – probably underestimated - ranges from 300 to 400 yrs. Regional tectonics is likely to have triggered most of the avulsions in the Morona-Pastaza area but its influence is restricted to this area. The factors controlling the avulsions in the Tigre-Corrientes area are less clear because the frequently described "hydrologic"-driven avulsion as observed in areas characterized by contrasted hydrologic cycles are inconsistent with the characteristics of the hydrologic cycles of the Rio Pastaza.

Keywords : Avulsion, megafan, Amazonia, controlling factors, post-LGM, tectonics

Introduction

Fluvial megafans form as rivers exit the topographic front of a mountain and play a major role in the dispersal of sediments and sedimentation in overfilled foreland basins (Leier et al. 2005).

Because of their size and mean slope, megafans constitute specific geomorphic units. Whereas smaller-sized alluvial fans involve deposition of successive lobes as the main process of sediment accumulation (Blair and McPherson 1992; Schumm et al. 1987), sedimentation in megafans is dominated by avulsion and bifurcation of the main streams (Bridge and Karssenberg, 2005). Style of avulsions (Slingerland and Smith, 2004) in megafans as well as their frequency strongly influences the sedimentation rate and the stratigraphic architecture. Numerous studies have been carried out on the typology and frequency of avulsion and characteristics of anastomosis in deltas (Törnqvist, 1994; Stouthamer and Berendsen, 2000; Stouthamer and Berendsen, 2001), and alluvial plains (Nelson, 1970; Saucier, 1994; Autin et al., 1991; Morozova and Smith, 1999; Morozova and Smith, 2000). Megafans have been less considered (Gole and Chitale, 1966; Gohain and Parkash, 1990; Singh et al., 1993; Assine, 2005; Assine and Soares, 2004). However, because of their size, slope and situation in the piedmont of mountain fronts, the question arises of the specificity of megafans in terms of causes and triggers of avulsion, and, in particular, the balance between tectonics and sedimentary/climatic events.

This study focuses on the Napo-Pastaza megafan in the northern Andes. This megafan is located on the Amazonian foothills of Ecuador and northern Peru, roughly between 2°00 and 5°00S and between 74°00W and 78°00W. It covers 51 400 km^2 (Fig. 1). This study is based on the mapping of the successive courses of the Rio Pastaza and its main tributaries, mainly from remote sensing and DEM analyses. The aim of this paper is to establish the relative chronology, the average frequency and the style of the avulsions in the past 20 000 yrs and to discuss the causes and triggers of these avulsions as functions of the different entities which have formed the megafan system. Dynamics of avulsion in the Pastaza megafan will be then compared with other areas known for frequent avulsions.

2 – General setting

2.1 – Geology and geomorphology

2.1.1. – Structural organization

The part of the Ecuadorian Andes involved in the Amazonian drainage can be divided into 4 morphotectonic

units which are, from west to east: the Western Cordillera, the Interandean depression, the Eastern Cordillera, the Subandean zone and the Amazonian foreland (Fig. 1).

The Western Cordillera and Interandean Depression are constituted by Upper Cretaceous-Paleogene formations, mainly andesitic (Reynaud et al., 1999; Lavenu et al. 1992; Kennerley 1980) unconformably overlain by neogene andesitic formations affected by late Miocene to early Pleistocene deformations (Lavenu et al., 1992; Barragan et al., 1996; Hungerbühler et al., 2002; Winkler et al., 2005) and Quaternary volcanic formations (Kennerley 1980; Barberi et al. 1988; Lavenu et al. 1992).

The Eastern Cordillera consists in Paleozoic through upper Cretaceous rocks, metamorphosed and deformed during late Cretaceous to Paleocene time (Pratt et al. 2005), eroded and then blanketed by late Miocene to Pliocene volcanic/volcanoclastic formations and Quaternary volcanics (Lavenu et al. 1992). Apatite fission track analyses and U-Th/He measurements indicate a moderate to slow uplift from the Miocene to the late Pliocene (Spikings et al., 2000; Spikings and Crowhurst, 2004).

The Subandean zone is separated from the Eastern Cordillera by the west dipping Subandean Thrust fault. The Subandean Zone comprises in the west the Abitagua Cordillera, and in the east two thrust-related antiformal thrust stacks (as defined by e.g. McClay, 1992), locally known as the Napo and Cutucu "uplifts", involving Jurassic through Neogene formations. These antiformal stacks appear as axial culminations (in the sense of Ramsay, 1967 p. 346, Ramsay & Huber, 1987) separated by an axial depression known as the Pastaza depression. The Pastaza depression is filled with middle (?) through Upper Pleistocene piedmont deposits (Mera formation) which formed the apex of the Mera megafan (Tschopp 1953; Baby et al. 1999; Bes de Berc et al. 2005).

In front of the Subandean Zone the Amazonian basin preserves a sedimentary stack ranging from Paleozoic to Oligocene overlying the Brazilian shield. Fluvial aggradation occurred there since ~ 22Ma accumulating sediments issued from the west (Christophoul et al. 2002; Burgos 2006) to build a very large megafan. This large megafan termed hereafter Neogene megafan corresponds to the present day basins of the left bank tributaries of the Rio Maranon (including the Rio Pastaza) and those of the right bank tributaries of the Rio Napo. It can be shown that the apex of this fan migrated eastward from the early Miocene to now as a result of the forward propagation of the mountain front (Christophoul et al., 2002; Bes de Berc et al., 2005; Burgos, 2006). In the east of the megafan, an elongated flat-topped topographic high striking N130°, interpreted to be the exhumed Upper Miocene forebulge (Iquitos Arch in Roddaz et al. 2005), appears as an area of no- or limited Neogene deposition. The active part of the megafan (the modern Pastaza megafan) is located in the south-western side of the Neogene megafan, including the left-bank tributaries of the Rio Morona-Santiago, the lower Rio Pastaza, and the right-bank tributaries of the Rios Tigre and Corrientes.

2.1.2 – The Puyo Plateau

The 'Pastaza depression' appears as a very gentle arch dipping 0.4-0.5° west in its central part known as the Puyo plateau. The plateau surface appears as a low angle weathered and hardened surface cut through the uppermost Pleistocene Mera megafan (Mera surface, Heine, 1994, Heine, 2000; Bes de Berc et al. 2005). The same surface is found in the upper Amazonian foreland (Villano surface, Fig. 1 and 2) here it forms another but highly dissected plateau. Arching and backtilting of the Puyo plateau as consequences of the propagation of the Subandean Frontal Thrust (Bes de Berc et al. 2005) caused beheading or diversions of the transverse rivers – including the Pastaza River – which formerly flowed eastward into the Amazonian plain (Bès de Berc et al. 2005; Burgos, 2006).The tectonic offset between the Puyo and Villano plateaus reaches ~450m in the centre of the arch and decreases progressively sideways. The Mera erosional surface formed between ~23-24 ^{14}C ky BP which is the age of the younger sediment cut by the surface, and ~18 ^{14}C ky BP which is the age of the older deposits along rivers incising the surface (Bès de Berc et al., 2005). As this period corresponds to the time of deposition of the Last Glacial Maximum (LGM) terminal moraines (Heine, 2000) the formation of the surface can be ascribed to the LGM. Therefore, arching and backtilting of this surface and the consecutive diversion of the Rio Pastaza were younger than the LGM.

2.1.3. – The Rio Pastaza catchment upstream of the Amazonian domain

The Rio Pastaza forms by the confluence of two longitudinal rivers flowing in the Interandean Depression (Fig.1 and 2). Downstream of this confluence, the Rio Pastaza crosses the Eastern Cordillera along a deep (> 2200 m) and narrow transverse valley (Fig. 1). In the Subandean Fault Zone and the western Puyo plateau, the Pastaza valley becomes much wider and shallow showing stepped degradational terraces (Bes de Berc et al. 2005). In the central Puyo plateau, the Rio Pastaza traverses a preserved Pliocene volcanic complex. The overall flow direction is there toward the south-southeast. The area of the Pastaza catchment upstream of its debouchement in the Amazonian plain is 13 700 km^2. Measurements of vertical incision rates in the Eastern Cordillera since the LGM have given values ranging from 0.5 to 0.67 cm year^{-1}, increasing from the LGM to now, resulting from a rapid uplift, up to 1 cm year^{-1} in front of the Abitagua cordillera (Bès de Berc et al., 2005). The deep incision of the Eastern Cordillera by the Pastaza valley indicates that a rather rapid uplift of at least 2 mm year^{-1} succeeded the Miocene through middle Pliocene period of slow denudation and uplift evidenced by the Apatite fission tracks analyses and U-Th/He measurements of Spiking et al. (2000) and Spiking and Crowhurst (2004). Denudation rate, greater than ~0.2 mm year^{-1} in average and locally as high as 0.4 mm year^{-1}, have been obtained in the Eastern Cordillera by Vanacker et al. (2007) from cosmogenic radionuclide (^{10}Be) studies.

2.2 – Climatic setting

2.2.1 – Late Pleistocene and Holocene climate

Several authors (Hastenrath, 1981; Hastenrath and Kutzbach, 1985; Heine and Heine, 1996; Heine, 2000) consider the LGM to have been a cooler and more arid period responsible for the lack of sediment in the Brazilian

lowland between 24 and 17 ky (Ledru et al.; 1998) whereas Seltzer et al. (2002) indicate cool but wet conditions from 30 to 15 ky in the Peruvian Altiplano. In Ecuador, the LGM moraines are ^{14}C dated between 25 and 15 ky although the maximum extent of glaciers is inferred to have occurred between 30 and 25 ^{14}C ky BP (Heine, 2000). According to the latter author, the retreat of glaciers between 25 and 16 ^{14}C ky BP was due to glacier shrink because of increased aridity (increased insolation and decreased precipitations) and not to warming (Heine, 2000). Increased aridity can explain the development of an erosion surface involving soil creeping and sheetflooding rather than fluvial incision and transport (e.g. Leeder et al., 1998). In the southern interandean depression, pollen analyses indicate that climate was cooler and moister than today during the late-glacial period (17 – 11 cal. ky BP, Rodbell et al., 1999; Hansen et al., 2003). However, the vegetational changes in the Interandean Depression may have been influenced by winds from the west as well as from the east (Hansen et al., 2003) and these results are not necessarily applicable to the Amazonian basin much more influenced by the humid Atlantic winds.

For Clapperton et al. (1997) a significant re-advance of glaciers occurred during the Younger Dryas (11 to 10 ^{14}C ky BP) whereas for Heine and Heine (1996) and Heine (2000) this advance of glaciers took place at least 500 years later.

The climatic data for the Holocene have been inferred from vegetational changesin the Interandean Depression (Rodbell et al., 1999; Hansen et al., 2003) and in the northern side of the Neogene megafan (Yasuni National Park, northeast of Ecuador, Weng et al., 2002). Weng et al.'s (2002) palynological studies indicate that tropical rain forest has developed throughout the Holocene with minor climatic oscillations. According to these authors, severe droughts occurred in the period 8700-5800 cal years BP, which should be correlated with other records from Amazonia, adjacent savannas and the Andes (Hastenrath and Kutzbach, 1985; Frost, 1988; Behling and Hooghiemstra, 1998, 1999). This "dry" period was succeeded by more uniform and wetter conditions with alternating wetter and drier millennial-scale events (Weng et al., 2002).

2.2.2 – The ENSO events

ENSO (El Nino Southern Oscillation) events have been recorded in Ecuador and neighbouring areas since the late Pleistocene. According to Keefer et al. (2003) studying deposits in the Pacific side of the Northern Peruvian Andes, 10 severe ENSO events occurred between 38,200 and 12,900 cal. years. In the southern Interandean Depression of Ecuador, Rodbell et al. (1999) and Moy et al. (2002) studying storm-induced lake deposits found that ENSO events became significant only after ~5 ky BP, with highest spectral density and frequencies between ~3.5 and 2.6 ky and during the last 660 years. The reduced ENSO activity should be correlated with the severe droughts of the period 8700-5800 cal years BP inferred by Weng et al. (2002) whereas the increased ENSO activity should be correlated with the following wetter period. The 17th and 20th centuries are also characterized by very strong ENSO events (Cobb et al. 2003; Keefer et al., 2003) and the last very severe events occurred in the years 1982-1983 and 1997-1998.

The recent and historical ENSO events generated floods and steep-sloping hillslope-toe landslides on the western slopes of the Western Cordillera, an area that is normally much less humid than the Eastern Cordillera and Amazon basin (Demoraes and d'Ercole, 2001). In contrast, in eastern Ecuador continuously submitted to the humid Atlantic winds no unusual floods were signalled during the 1982-1983 and 1997-1998 events. Similarly, no catastrophic floods have been registered for the 17th century events in the catalogue of major historical disasters in eastern Ecuador with the reserve that chronicles of that time seem to have been little concerned with eastern Ecuador.

2.3 – Tectonic activity

2.3.1 – Recent and active tectonics

In the Interandean Depression, late Miocene to early Pleistocene syntectonic deposits have been recognized and dated by means of K-Ar and U-Th/He measurements at 8.5 – 7.9 Ma to 1 Ma (Lavenu et al., 1992; Kennerley, 1980; Barberi et al., 1988; Barragan et al., 1996; Hungerbühler et al., 1995; Winkler et al., 2005).

In the Eastern Cordillera, the deformation affects the widespread volcanic and volcaniclastic Pisayambo formation aged of 9-10 to 6 Ma (Lavenu et al., 1992; Barberi et al., 1988), and lavas issued from volcano Altar aged of less than 3.5 Ma (Lavenu et al., 1992), which indicates that the deformation is younger than 3.5 Ma. Apatite fission track analyses and U-Th/He measurements in the western Eastern Cordillera indicate a slow to very slow (when compared with other active ranges) denudation rates from the Miocene to the late Pliocene/early Pleistocene (Spikings et al., 2000; Spikings and Crowhurst, 2004). Since the Rio Pastaza has incised the eastern Cordillera more than 2000m (Fig.1), these results support the interpretation that deformation and related uplift of the Eastern Cordillera was Pleistocene in age.

In the frontal Eastern Cordillera and the Subandean Zone, a tectono-sedimentary and geomorphic study supported by ^{14}C dating indicate a tectonic activity related to the propagation of a low angle thrust ramp from at least the middle Pleistocene to now (Bès de Berc et al., 2005).

2.3.2 – Earthquakes

In the Harvard Catalog 30 earthquakes with magnitude Mw ≥ 5 were registered between 1976 and 1999 in eastern Ecuador, with two events ≥ Mw7 (Mw7.1, 03/06/87; Mw7.0, 10/03/95), the latter being attributed to the activity of the Cutucu frontal thrust (Yepes et al., 1996). 30 historical events with intensity ≥ VIII have been recorded between AD1541 and AD 1995 (IGEPN, 1999). One event of intensity XI has occurred in AD1797 (MsNOAA magnitude 8.30, NOAA Catalog, U.S. Geological Survey, 2003), and two events of intensity X in AD1698 (MsNOAA magnitude 7.70) and AD1949 (MsNOAA magnitude 6.80). Most of these events are situated in the Eastern Cordillera and the Subandean Zone. The rare events situated under the Pastaza megafan were deep events which are likely to have had no influence on the drainage network.

2.4 – Landslides

Earthquakes-triggered landslides were observed in the Eastern Cordillera such as those triggered by the 5 March 1987 M~7 event (Hall, 1991). In eastern Ecuador, the major landslides not triggered by earthquakes were independent of the ENSO events (for example, the La Josefina landslide, the greatest known in Ecuador, occurred in 1993, Demoraes and D'Ercole, 2001). Moreover, no landslides related to the severe and frequent 17th century ENSO events are registered in the catalogue of major historical disasters and no landslide formed during the 1982-1983 and 1997-1998 events (Demoraes and D'Ercole, 2001). Whatever their trigger, the sediments delivered by these major landslides were incised and entirely removed by rivers a few days after the disaster (e.g. Hall, 1991) with no avulsion observed downstream. In any event, no major landslides have been registered in the valleys of the Rio Pastaza and major tributaries, and a careful observation of satellite images and air photos has shown no well characterized landslide scars in the upper Pastaza basin.

2.5 – Volcanic eruptions

Ecuador is characterized by 20 active volcanoes (e.g. Hall, 1977; Hall and Beate, 1991; Hall et al., 2008). Four of the most important active or recently active volcanoes, Chimborazo, Cotopaxi, Tungurahua, and Sangay are within, or at the boundary of, the Pastaza drainage basin (Fig.1).

Chimborazo volcano was active in the late Pleistocene (Hall and Beate 1991; Barba et al., 2008) and the Holocene (between about 8000 and 1000 years ago, Barba et al., 2008). The first two of the major Holocene events generated large pyroclastic deposits and thick lahars. Pyroclastic deposits are described for 5 other major eruptions occurring until the 5th to 7th centuries (Barba et al., 2008).

Cotopaxi volcano had numerous eruptions producing andesitic scoria and pumice ash flows, blocky lava flows, and lahars (~30 eruptions since 1530, Hall, 1977). At least four rhyolitic eruptions occurred during the past 10 000 years. A very large (~71 000 m^3) debris flow (lahar) occurring ~4500 years ago flowed >130 km east and south into the Rio Patate valley. The initial dry volume has been estimated to ~2 km^3. The most distinctive lahar deposits of the historical period occurred in 1877 and in the 18th century. Since 1906 only small eruptions are signalled with limited ash falls or pyroclastic flows (IGEPN, 2009) although renewed seismic activity has occurred since 2001 (Molina et al., 2008). Modelling of lahar flows indicate high discharge rates (~15,000 m^{3}s^{-1}, Castro et al., 2006).

Tungurahua volcano has been active since at least the late Pleistocene. Tungurahua II, mainly composed of andesite lava flows younger than 14 ky BP, was partly destroyed by a collapse event, 2955 ± 90 years ago, which produced a 8-km3 avalanche on a distance of ~ 20 km and a large lahar (Hall et al., 1999). The eruptive activity of the present volcano (Tungarahua III) commenced in the period ~2300 – 1400 years BP (Hall et al., 1999). Lava extrusions and pyroclastic flows occurred since the 14th century, notably in 1773, 1886, 1916-18 and 2006-08 (Le Pennec et al., 2008; IGEPN, 2009). During the 1916 and 1918 eruptions, large amounts of ashes and lapillis were transported by Pastaza's tributaries (IGEPN, 2009). An ash layer of ~6x10^{6}m^3 was deposited in August 2001 near Baños and the Patate/Chambo confluence (Le Pennec et al., 2008).

Sangay volcano is the most active volcano in the Northern Vocanic Zone of the Andes and a permanent explosive activity has been observed since 1628 with an average recurrence time of large eruptions of less than 50 years. The early Sangay III lava flows are older than LGM moraines (Monzier et al. 1999). The activity is of a Strombolian type with block and ash explosions, ash falls, pyroclastic flows and lahars (see Monzier et al., 1999).

The direct impact of these eruptions on the Amazonian Pastaza system is difficult to appreciate. For example, the 4500 years-old lahars generated at the Cotopaxi cap, although gigantic, are not observed downstream of the Patate – Chambo confluence. The lahars produced by the 3000 years BP sector collapse of the Tungurahua have been observed in none of the terraces of the Rio Pastaza downstream of the immediate proximity of the volcano (Bès de Berc et al., 2005). The large historical pyroclastic flows of the Tungurahua have been largely contained within the channel cut by a tributary to the Pastaza and did not reach this river (Stinton and Sheridan, 2008). However, in the upper Pastaza valley, near Baños, the T2 terrace covered with a lava flow dated between ~2200 and ~1500 ^{14}C years BP (Hall et al., 1999) overlies fluvial deposits made of reworked volcanic material (Bès de Berc et al., 2005). Volcanic material reworked by fluvial transport has also been observed in a low terrace cut into the Middle Pleistocene volcanic hills of the Puyo plateau (Burgos et al., unpublished). Deposits from the eastern flank of Sangay III have been stocked in the Sangay fan (Monzier et al., 1999) and it is unlikely that more than a minor part of these deposits was introduced en masse into the Pastaza network after each eruption.

The volume of material input by the volcanic eruptions in the Pastaza network is more difficult to estimate because only the volume of exceptional or recent events has been calculated. The volumes of material for these exceptional events are ~<2 km^3 for the Chimborazo; 2.5 km^3 for the Cotopaxi giant lahar to which could be added a volume of ~4 km^3 representing the 4 rhyolitic eruptions signalled by Mothes et al. (1998); the ~3000 years BP sector collapse of the Tungurahua II mobilized 8 km^3 to which could be added associated lahars. The numerous eruptions of lesser importance mobilized much smaller volumes of material. If we assume that each of these eruptions provided approximately the same quantity of material as the 2006 eruption (~5 10^{-3} km^3), and that the frequency of eruptions has remained similar to that of the historical ones, then the 30 eruptions have given no more than ~0.15 km^3. This gives a total volume of less than 20 km^3 to which must be added the volume of the Sangay deposits which have not been stocked in the Sangay fan.

3 – Material and Methods

The avulsions in the Pastaza megafan have been studied by means of remote sensing image analysis because of its size and of the inaccessibility of the greatest part of the area. Moreover, the high density of the vegetation and the low topographic amplitude of alluvial ridges make field identification of abandoned fluvial

morphologies difficult.

This study was performed using Landsat and ASTER images and SRTM DEM. The set of Landsat images used in this study is summarized in Table 1.

The MrSID™ Landsat 7 images, correspond to a mozaic of 58 images acquired on a period ranging from 1999 to 2001 (see Table 1). These mozaics extend north-south over 10 degrees of latitude, and span east-west for the full width of the UTM zone.

These images are processed to change the Landsat spatial resolution (30m) of the multispectral composition. First, TM7 Band (midle-infrared), is displayed as red, TM4 band, near-infrared band, is displayed as blue and TM2 band, green band, is displayed as green.

The initial pixel size of these bands (~30m) is then reduced using cubic interpolation to the spatial resolution of the panchromatic band (TM8, ~15 m).

The process follows with calculation of the Hue-Saturation-Intensity schemes for the multispectral images. The multispectral image is reconstructed from the Hue-Saturation schemes and the intensity scheme is replaced by the TM8 panchromatic band. The resulting sharpened image combines the spatial resolution of the panchromatic band (~15m) with the radiometric characteristics of the 30 meter data, which allows the preservation of high frequency details.

MrSID Landsat 5 images have a lower resolution of around 30m. The mosaic corresponds to 78 images with a period ranging from 1986 to 1994 (Table 1).

For detection of soil moisture and vegetation changes we used ASTER images that have higher accuracy. This sensor acquires four bands on VNIR spectral domain, 6 band on the short-wave infrared (SWIR) and 5 band on the Thermal domain (TIR). The spatial resolution of the sensor decrease with the wavelength: 15m on VNIR domain, 30m on SWIR and 90m in thermal domain. As for Landsat 7 image, the SWIR and TIR resolution was improved using the same process of image sharpening using high spatial resolution of VNIR bands (i.e. 15m).

The spectral response of vegetation is characterized by a high reflectance level in the near-infrared region (NIR from 700 to 1400 nm, Baret and Guyot 1991). In western Amazonia, botanical studies have determined that changes in the abundance of vegetation (palm flora) are related to topography and soil drainage conditions (Montufar and Pintaud, 2006).

Vegetational changes are organized in very bright, more or less sinuous, bands, ~1 kilometre-wide and 10 to 100 kilometres long like those shown in Figure 3. These narrow and sinuous bands are interpreted as abandoned streams along which vegetation is absent or recent. The absence or the recent development of vegetation may be a result of the recent abandonment. Vegetational changes may have also been caused by changes in the draining properties of soils due to the presence of coarser-grained sedimentary bodies such as channels and alluvial ridges.

We used also radar images which have interesting capabilities of vegetation penetration of the microwaves. This penetration capability increased with the wavelength, in our studied area ground penetration can not occur due to soil moisture. In some case, when the gallery forest covers abandoned channels we used JERS radar images which permit to evidence hidden fluvial channels for the optical (s.l.) Landsat and Aster images. Another interesting property of the radar wave penetration is its capacity to cross the clouds.

To supplement this study we also used the Shuttle Radar Topography Mission DEM (SRTM V3 with three arc second of spatial resolution). Its vertical accuracy is around 10-15m depending on topographic gradient, vegetation cover, tropospheric humidity (Welch and Marko 1981; Lang and Welch, 1994).

Geomorphologic studies using SRTM data have demonstrated its efficiency (Potts et al., 2008; Zandbergen, 2008; Guth, 2006 and among others). For Amazonian morphology, Rosseti and Valeriano (2007) starting from the example of the Amazon estuary in Brazil demonstrate the pertinence of using SRTM DEMs for mapping abandoned streams and other geomorphic features in low relief, highly vegetated, low areas such as rain forests.

4 – The modern Pastaza megafan complex

The present-day Pastaza megafan is situated in the southwest side of the Neogene megafan to the southeast of the Puyo plateau and covers 51 400 km^2, which is an area much larger than that of the catchment of the Rio Pastaza (13 700 km^2, see above). The Pastaza megafan appears as a marked topographic high within the Amazonian plain. In this respect, it is similar to the smaller-sized megafans identified in the Bolivian piedmont (Horton and DeCelles 2001), and differs from most of the distributary areas of the Amazonian lowlands such as the Rio Beni plain in Bolivia (Dumont 1996) which are depressed areas.

The modern megafan complex is bounded by the Rio Mangosiza/Morona to the west, the upper Rio Tigre valley and the Iquitos arch to the northeast, and the Rio Marañon to the south (Fig. 1). This megafan is formed by the left-bank tributaries of the Rio Mangosiza/Morona, the lower Pastaza basin, the lower Corrientes and lowermost Tigre basin (downstream of the Tigre – Corrientes confluence), and the tributaries to the Rio Marañon situated in the triangle between the Pastaza and Tigre/Corrientes basins.

The apex of the megafan complex is situated at the debouchement of the Rio Pastaza from the Puyo plateau (Fig. 1). The proximal part of the fan has a 3 $m.km^{-1}$ mean slope whereas, in the same area, the Rio Pastaza has a lower slope of 2 $m.km^{-1}$ (C in Fig. 4). There, the Rio Pastaza has an overall NW-SE direction and exhibits a multi-channel pattern with a high braiding parameter. In front of the Cutucu dome (Cangaime anticline), all the streams between the Rios Mangosiza and Cangaime, either tributaries to the Pastaza or to the Mangosiza/ Morona, exhibit a more or less accentuated curved pattern. This region will be termed hereafter Mangosiza-Cangaime area (MCA), (Fig.1, 2 and 4).

The middle part of the megafan system has a 0.5 $m.km^{-1}$ slope and the Rio Pastaza has a 0.3 m/km slope (reach D on Fig. 6). The Rio Pastaza is there a single channel low sinuosity meandering stream flowing toward the south. The change in flow direction of the Rio Pastaza from southeast to south will be termed hereafter the "Great Diversion of the Rio Pastaza" (GDP), (Fig.1and 8)

In this middle megafan complex, three regions may be distinguished. In the southwest, a parallelogram-shaped abandoned megafan well-apparent in the Landsat images

constitutes the present day drainage divide between the Morona and Pastaza basins (Fig.1). This region will be termed hereafter Morona Pastaza Area (MPA). In the southeast, another system, partly abandoned, includes the present-day lower Corrientes /Tigre basins. This region will be termed Tigre-Corrientes area (TCA). Between the MPA and the TCA, a large WNW-ESE-trending abandoned flood plain join the upper southeast-flowing reach of the Rio Pastaza to the Rio Corrientes. This area will be termed Pastaza-Corrientes transition band (PCTB). The NW-SE section of the modern Pastaza valley having the same direction as this abandoned floodplain and showing similar abandoned alluvial ridges is to be included in the PCTB.

The distal part of the megafan complex consists in a huge floodplain made of swamps, forested areas and open water areas with a very low regional slope (0.3 $m.km^{-1}$) and river slope (0.2 $m.km^{-1}$). In this distal fan part the Rio Pastaza exhibits an anastomosing pattern (Fig. 4, reach E). Its course is there markedly oblique to the general stream direction which is south-southeast to southeast. The lower order streams form anastomosed channels but remnants of former meandering reaches are frequently observed.

5 – Avulsions in the Pastaza Megafan complex

Numerous avulsions have been recognized in the different areas defined in the modern Pastaza fan (Figs. 2).

5.1 – Avulsion relics in the MPA

The MPA corresponds to the elongated abandoned megafan now forming the drainage divide between the Morona and Pastaza basins well apparent in the satellite images. The active streams that reoccupied some of the abandoned channels are still arranged as a low angle distributary pattern rising from the megafan ridge. The area of the abandoned alluvial fan is~13,750 km^2, greater than the well-known Kosi megafan, northern India, which is only ~10,000 km^2. Volume estimate by means of an integration of transverse profiles yields a minimum value of 140 km^3. The MPA fan apex is situated in the north-northwest, at ~30 km to the south of the modern Rio Pastaza in the area then occupied by the curved streams of the eastern MCA. In the northwest (Fig. 3A), paleochannels are amalgamated and difficult to distinguish in Landsat images and SRTM DEM unless where re-occupied by active streams. There, alluvial ridges appear quite rectilinear (3 on Fig. 3A). Meander loops are visible (2 on Fig. 3A) but their sinuosity is moderate (2 in Fig. 3A) and constant over the whole area (S~1.2).

In the median part of the MPA fan (3 on Fig. 3A), the paleochannels are not amalgamated and the morphology of alluvial ridges is much easier to characterize. Ancient streams display sub-parallel patterns and are frequently reoccupied by right bank tributaries of the modern Pastaza and the left-bank tributaries of the modern Rio Morona (Fig. 1 and 3C). Three types of reaches may be observed: (1) ancient reaches characterised by a reduced contrast between the valley and the forested floodplain; (2) recently abandoned reaches with a marked contrast between valley and floodplain; (3) abandoned reaches re-annexed, entirely or partly, by present-day rivers. These channels/alluvial ridges have a moderate sinuosity (but the modern streams that reoccupy these channels are much more sinuous), diverging channels are frequent and may have switched into adjacent ones (2 on Fig. 3A) as frequently observed in alluvial megafans (e.g. Wells and Dorr, 1987, in the Kosi megafan). True rejoining channels (*i.e.*, channels rejoining those channels from which they diverged *see* Slingerland and Smith, 2004) are rare. 44 avulsion sites involving two recently abandoned reaches or involving recently abandoned and presently active reaches have been numbered in the MPA (Fig. 3). Avulsion sites between older reaches or difficult to locate are mapped as 'supposed avulsion sites'. 12 of these 'supposed' avulsion sites have been numbered in the MPA.

In the south where slopes are shallower, diverging/rejoining channels forming anastomosed patterns are observed, in particular the lowermost Pastaza River. Swampy areas are frequent in this area except a topographically higher triangular plateau close to the Pastaza-Marañon confluence representing a remnant of the Villano surface.

5.2 – Avulsion relics in the MCA

In this area, the abandoned channels of the Rio Pastaza are numerous and identified using radiometric contrasts in the vegetation. Ancient alluvial ridges have been re-annexed by underfit streams, which makes easier their identification in the SRTM DEM. Re-occupation of pre-existing channels by underfit stream has been described as characteristic of a post-avulsion evolution of an abandoned reach (Bristow 1999).

The area to the east of the Cangaime anticline is characterised by a southward regional slope and a gently domed topography (Fig. 5). The principal rivers which appear as underfit streams having annexed ancient alluvial ridges describe a curved path around the forelimb of the anticline, those situated in the west incising the frontal dome and those in the east contouring it (1 on Fig. 3A and Fig. 6A). Incisions by these rivers are equal to, or exceed 10 m (Fig. 5). The rivers in the south west are issued from the west or the northwest and traverse the Cangaime anticline through transverse water gaps. The rivers situated in the centre or in the west of the dome are issued from the north of the anticline, in the area separating the anticline from the Puyo plateau, near the debouchement of the Pastaza. Several abandoned paths of the Rio Pastaza have been recognized in this area. Path #1 (Fig 6A and B) appears as a gentle convex to east curve parallel to the anticlinal front. This path is the oldest one, for it joins the highest terrace on the right bank of the Rio Pastaza. Its uppermost part cut the nose of the Cangaime fold through a water gap. This water gap is abandoned at the junction with the upper terrace where it is prolonged by a wind gap. Path # 1, except its uppermost part (the wind gap) is now reoccupied by the Rio Macuma which comes from the Eastern Cordillera after having formed a 180° loop at the tip of the western Cutucu dome (Bès de Berc, 2003). Path #2 (Fig. 6) leaves path #1 immediately to the south (Fig. 6A) and forms a tighter valley rejoining path #1 ~30 km downstream. Path #3 is derived from path 1 through an avulsion site located upstream of the 1-2 site (a in Fig. 6A). Another avulsive branch leaves path # 2 at point b to follow a new course which corresponds to a section of the present-day Rio Pastaza flowing toward the east-southeast (path # 4). Near point c, another abandoned stream is observed connecting the Pastaza and path #3 (path # 4).

The present course of the Pastaza toward the southeast (path # 5) thus appears as a result of the last avulsion. In any event, avulsion 4 (point c) was younger than avulsions 1 to 3, for the bifurcation between paths #4 and #5 is observed on a lower terrace. Paths # 1, # 4, and # 5 follow meandering valleys whereas path # 3 forms a low sinuosity valley. This low sinuosity valley contrasts with the high sinuosity and the low amplitude of the meander loops of the underfit stream which reoccupied it. No wide valley seems to have been ever formed by path # 2 but a series of curved tributaries is observed in LANDSAT images suggesting repeated partial avulsions giving rise to short-lived avulsive streams. The wide meanders of path # 4 having amplitude and bed width of the same order of magnitude as the present channel but higher sinuosity are well apparent in the LANDSAT images and the SRTM DEM at the vicinity (~8 km) of the present course of the Pastaza (path # 5). Meander mosaics preserving preferentially meander loops convex to the west are observed locally in the west of path # 4 whereas a vegetated band free of meander (Fig. 1) remnants separates path # 4 and path # 5 (the present Rio Pastaza).

5.3 – The avulsions in the PCTB and the Great Diversion of the Pastaza

Landsat images and the transverse profiles extracted from the SRTM DEM (Fig. 5) show that a large WNW-ESE-trending abandoned valley joins the upper southeast-flowing reach of the Rio Pastaza to the Rio Corrientes in continuation of the Pastaza valley. Downstream, *i.e.*, south of the GDP (Fig. 2 and 7), the Pastaza valley narrows significantly, which confirms the abandon of the former wide valley which assured the transition between the MPA/MCA and the TCA. As in the northern TCA, a succession of avulsions and channel rejoinings formed anastomosed channel patterns, now abandoned, in the present Pastaza floodplain as well as in the Pastaza-Corrientes abandoned valley. The multi-channel pattern shown by the present-day Pastaza in this area (downstream of the GDP) may represent the last expression of this process. Therefore, the PCTB, including the NW-SE reach of the Pastaza can be considered as an avulsion belt (Slingerland and Smith, 2004). It is worth nothing that the multi-channel pattern of the Pastaza disappears downstream of the abandon and the Rio Pastaza resumes a meandering course for an along-valley distance of more than 150 km.

In the east of the PCTB, 8 avulsion sites including the 4 ones having led to the present-day course of the Pastaza have been defined. In the west, 7 avulsion sites have been defined. The present southward bend of the Pastaza (GDP) resulted from the last of these avulsions (Fig. 1).

Immediately downstream GDP, the 1990 Landsat image (Fig.1) shows an oxbow-shaped swampy area appearing in a blue-green colour in the outer arc of the present-day bend, in geometrical continuity with the abandoned valley. This feature, less apparent in the 2000 image, suggests an ancient left-hand open curve cut through by the Pastaza. The SRTM DEM indicates that the bottom of the present Pastaza valley is there lower than the swampy area. A similar though smaller-sized feature is observed 25 km to the south (Fig.1). There, the present Pastaza channel diverged from a convex-eastward loop appearing in a bright light green to form a convex-westward curve flowing close to the abandoned channel without rejoining it. In both cases, the Pastaza thus appears as having incised through its proper valley to achieve the avulsion (avulsion by incision after Slingerland and Smith, 2004). It should be pointed out that downstream of the PCTB, the DEM profiles and the presence of swampy areas on both sides of the river bed indicate that the Rio Pastaza exhausted its bed instead of incising it as in the north. This uplift of the Pastaza has for effect to separate the eastern portions of previous southeast-flowing rivers now dying out into the swampy fringes of the right side of the Pastaza alluvial ridge from their western counterpart now rising from the swamps of the left side of this ridge.

5.4 – Avulsions in the TCA

The TCA is composed of two parts. The northern part (upper and middle Corrientes) shows distributary / rejoining alluvial ridges settled in a wide (up to ~70 km) floodplain, giving rise to anastomosing channels which characterize partial avulsions (*see* definitions and terminology in Slingerland and Smith, 2004). The modern and ancient alluvial ridges are distinguished by contrasted spectral responses as shown by the example of the Rio Corrientes at the vicinity of the north-eastern boundary of the area (Fig. 3B). Abandoned alluvial ridges (1 and 2 in Fig. 3B) have in general a brighter response and sharp boundaries strongly suggesting that vegetation was younger, and therefore that the avulsions were younger, than in the MPA. The abandoned channels, however, have a more or less bright green response (indicating a more or less recent vegetation growth) which can be interpreted as a succession of abandonments and avulsions. The alluvial ridges in the TCA are linear as in the MPA but the sinuosity of the ancient channels seems to have been higher (~1.7). Recent meandering streams such as the modern Rio Corrientes may reoccupy the larger abandoned channels (3 in Fig. 3B). 18 avulsions sites have been numbered in this northern part of the TCA. In the middle part of the TCA two avulsion belts may be distinguished: the lowermost Rio Corrientes belt trending west-east in the northeast and the Cuinico belt trending northwest – southeast in the southwest.

The southern part of the TCA is fan shaped showing modern and ancient distributaries joining the Rio Marañon or the lowermost Rio Tigre. Landsat images show two interfering fans well apparent in the arrangement and shape of the numerous swamps of this region (Fig. 1). This pattern is less obvious, however, when only the alluvial ridges and well defined channels are considered (Figs. 1 and 3).The modern and abandoned channels are mostly parallel, even though more sinuous channels are observed in the upper part. Well-characterized avulsions are less frequent than in the north (9 avulsion sites) even though some of the channels are anastomosed.

6– Chronology, age and frequency of avulsions

The observations above may arrive to a relative chronology of the major avulsions. The radiocarbon ages available in the literature (Räsänen et al. 1992; Räsänen et al. 1990; Bes de Berc et al. 2005) help us to constrain the ages of the avulsions in the areas of the Megafan. In the

entire Pastaza megafan complex, 108 avulsion sites have been identified, representing an avulsion frequency of 0.51±0.06 / 100 years and an average recurrence time of ~200 years (196±2yrs and 240±3yrs if we except the 'supposed' avulsion sites) (Table 2). However, as shown above, the type and origin of avulsions are quite different in the areas we have distinguished and this value is only indicative.

6.1 – Avulsions in the MCA/MPA and western PCTB

The first entity to have developed was the MPA megafan (Fig. 8A) where the channels, though re-annexed, were abandoned a long time ago as shown by their subdued spectral response. The brighter spectral response of the abandoned channels in the TCA indicates that the abandon was younger than in the MPA. This is confirmed by the fact that the eastward avulsions in the MCA from which originated the channels of the PCTB area and the TCA derived from the southward-flowing paleo-Pastaza which fed the MPA megafan. The curved streams of the MCA appear to be superimposed on the apex of the MPA megafan and can be thus considered to be younger. In terms of ages, the apex of the MPA megafan being situated at the debouchement of the Rio Pastaza from the Puyo plateau, the formation of this megafan and the avulsions therein are younger than the diversion of the Pastaza in the Puyo plateau. This diversion being a result of arching and backtilting of the plateau surface (Mera surface), the MPA megafan was younger than 17,920±100 ^{14}C years BP (Bes de Berc et al., 2005), or ~21,160±260 cal. years BP according to Reimer et al.'s(2004) IntCal calibration.

The relative chronology between the MCA and the PCTB avulsions is less easy to establish. However, if we take into account the chronology of avulsions and the outward progression of the curved stream network pattern in the MCA on one hand and the chronology of avulsions in the western PCTB on another hand, it appears that the last diversion in the MCA corresponds to the first diversion in the PCTB (Fig. 8B). Therefore, one can consider that the avulsions in the MCA are older than those in the TCA. Ages of 9200±200yrs and 8480±110 Cal yrs BP have been obtained by (Räsänen et al. 1992) in the floodplain of the Rio Corrientes in the northern TCA. The development of this floodplain being a result of the avulsions at the origin of the TCA, the abandon of the MPA was older than 9200±200yrs Cal yrs BP.

If we group the avulsions older than the first occupation of the TCA floodplain, i.e., those in the MPA, the MCA, and the PCTB, 84 avulsion sites have been defined, including 17 'supposed' sites. If the date of 8480±110 Cal. years BP is considered as the age of the first occupation, then the frequency is ~0.66±0.2 / 100 years and the recurrence time is ~150 years (142±6 years accepting all sites and 179±7 years excepting the 'supposed' sites). Assuming a first occupation age of 9200±200 Cal. years BP, the frequency is ~0.7 / 100 years and the recurrence time is ~170 years (151 ± 4 yrs accepting all sites and 189±6 yrs excepting the 'supposed sites').

6.2 – Avulsion in the TCA, eastern PCTB and modern Pastaza

As shown above, avulsions in the TCA occurred around 9200±200 Cal. years BP and 8480±110 Cal. years BP, The last avulsion to occur in the PCTB was the diversion to the south of the Pastaza "Great Diversion" leading to the abandon of the eastern PCTB and the TCA (Fig. 8D). As a consequence, Avulsions in the eastern PCTB are supposed to have occurred after the last avulsions in the TCA (8480±110 Cal. years BP). The overall present-day course (and thus the "great diversion") of the Pastaza is figurate in a map published in 1691 (Samuel Fritz map reproduced by Gomez 1994), indicating that the "Great Diversion" was older than AD 1691.

In the TCA and the eastern PCTB, 26 avulsion sites have been numbered. If the date of 8480±110 cal. years BP was that of the first occupation of the eastern PCTB and TCA and the date of 1691 AD that of the last avulsion, the avulsion frequency were ~0.31 / 100 years and the recurrence time reduces to ~350 years (342±5 years for all sites to 391±6 years accepting the 'supposed' sites). If the age of first occupation of the eastern PCTB and TCA were 9200±200 Cal yrs BP, then the average frequency of avulsions were 0.29 / 100 years and the time of recurrence were ~400 years (372±9 yrs for all sites and 426±10 yrs excepting the 'supposed' sites).

The present day activity of the underfit streams reoccupying the pre-existing channels of the TCA is due to the fact that these streams have been re-alimented by streams newly formed in the upper Villano surface in front of the Puyo landslides (including the Rios Tigre and Corrientes, Bès de Berc et al., 2005). The relatively recent age of the Pastaza "Great Diversion" is also attested by the beheading of the SW-flowing rivers formed after the abandon of the MPA megafan.

6.3 – Significance of frequencies

The frequencies and average recurrence times of the avulsions in the TCA appears to be significant because of the homogeneity of the area and the similarity of the avulsion features. In contrast, the avulsions older than the occupation of the TCA floodplain formed in at least 3 differing contexts: construction of an alluvial megafan (MPA), piedmont of a propagating thrust-related fold (MCA), and construction of an avulsion belt (PCTB). Therefore, it is likely that the mean recurrence time varied from one area to another, and the average time of ~350 years can be considered as an order of magnitude.

7 – Discussion

7.1 - Avulsion frequency

Data relating to avulsions frequency exist for a few modern rivers in various contexts including avulsion belts, megafans, and deltas. Stouthamer and Berendsen (2001, table 2) present such data as interavulsion periods (= period of channel activity minus avulsion duration). Because our study cannot provide neither avulsion duration nor the number of coeval avulsions, interavulsion periods cannot be determined and the recurrence time referred to in the present paper assumes 'instantaneous' avulsions. Average frequencies (= total number of avulsions having occurred during a given period divided by the duration of this period) being independent of the duration of the avulsions have been preferred in the following discussion. Table 3 presents average frequencies in the areas

considered by Stouthamer and Berendsen (2001) to which have been added the Brahmaputra River (Bristow, 1999) and the Taquari megafan (Assine, 2005).

The average avulsion frequency of 0.51 / 100 years for the whole Pastaza megafan complex is of the same order of magnitude as for the Rhine-Meuse delta (0.88/ 100 cal years, Stouthamer and Berendsen, 2001) but much less than for the Lower Brahmaputra River (3.47, Bristow, 1999), the Kosi megafan (4.88, Gole and Chitale, 1966), or the Taquari megafan (~10, Assine, 2005) which have, however, been observed during much shorter periods of time (202, 246, and 30 years, respectively, see Table). In contrast, this avulsion frequency of 0.51 / 100 years is greater than those of the Saskatchewan River (0.17, Morozova and Smith, 1999, 2000), the Po River (0.25, Nelson 1970 *in* Mackey and Bridge, 1995) or the Yellow River (0.21, Li and Finlayson, 1993).

When considering the different entities constituting the Pastaza megafan complex, the western domain formed by the MPA, the MCA, and the western PCTB records a higher avulsion frequency (~0.6-0.7) than the eastern domain (~0.3). The former value is probably underestimated because many older channels in the MPA are likely to have been masked by the large aggradation having occurred in this area. A comparison between the MPA megafan and the other megafans (Kosi, Taquari) is difficult because we have no age for the MPA alone and the situation or geometry of these megafans differs markedly. The Kosi megafan appears as a piedmont megafan like the MPA but it is very flat compared with the MPA and is affected by a monsoonal climate. This may allow the mechanism proposed by Wells and Dorr (1987) to operate in this megafan and not in the more bulging MPA, thus explaining the much higher avulsion frequency in the former. In fact, the avulsion frequency in the MPA is the closest to that in the Rhine-Meuse delta which has formed in a much different context but is closely controlled by aggradation (Stouthamer and Berendsen, 2000, 2001).

The value obtained in the PCTB-northern PCA floodplain avulsion belt is very close to those obtained in floodplain avulsion belts having similar areas (Saskatchewan and Po Rivers) or much larger areas (Yellow River) during similar spans of time but much lower than in the Brahmaputra floodplain, which has, however, been observed during a much shorter period. This suggests that the avulsions forming avulsion belts in low gradient floodplains might have similar long-term average frequencies, but highly varying short-term average frequencies. In this respect, floodplain avulsion belts should be similar to deltas such as the Rhine-Meuse where avulsion frequency varies in the time from 2.43 between 8000 and 7300 cal years BP to 0.85 between 7300 and 3200 cal years BP (Stouthamer and Berendsen, 2001).

7.2 – Style, local causes and triggers of avulsions in the Pastaza megafan complex

The origin of avulsions have been thoroughly discussed by Jones and Schumm (1999) and Singerland and Smith (2004) in their reviews of river avulsions.

Jones and Schumm (1999) consider 4 groups of causes and eventually triggers of avulsion. The first two groups involve an increase of the ratio of the slope of the potential avulsion course to the slope of the existing channels. The third group involves a reduction in the capacity of a channel to convey all of the water and sediment delivered to it. The fourth group involves other processes than those of groups 1 to 3, as various as animal trails and stream capture. In the context of the Amazonian basin, the group 4 processes are precluded or unlikely. Intrinsic processes related to sedimentation and extrinsic (external) processes are involved in any of the groups 1 to 3. External processes such as tectonic uplift/subsidence or lateral tilting are thought by Jones and Schumm (1999) to be capable of causing (and not only triggering) avulsion. Slingerland and Smith (2004) used a theoretical stability analysis of bifurcating channels and a thorough review of the papers dealing with the style and frequency of avulsions. They concluded that avulsion frequency increases with increasing aggradation whatever the exact cause of aggradation and the trigger (even though the authors acknowledged that avulsions may occur in the case of limited or no aggradation). According to them, avulsions are promoted by rapid alluviation of the main channel, a wide unobstructed floodplain able to drain down-valley, and frequently recurring floods of high magnitude. According to this viewpoint, it should be appealing in a megafan to distinguish between causes and triggers of avulsions. In this case, the cause should be the huge amount of sediment transported into the megafan (see e.g. Wells and Dorr, 1987, or Leier et al., 2005), and the trigger should be “opportunistic” (Slingerland and Smith, 2004), intrinsic (e.g. high floods) as well as extrinsic (e.g. tectonics). Accordingly, only the cause of the high sedimentary load should be researched as the cause of the avulsions in the entire modern Pastaza megafan complex, tectonic events being considered as opportunistic triggers. However, Jones and Schumm (1999, their table 1) consider tectonics as a cause as well as a trigger of avulsion because tectonic uplift may decrease channel slope or increase the slope of the potential avulsion course as this is obvious in the case of piggy back basins formed upstream of growing anticlines (see e.g. Burbank et al., 1996; Burbank and Anderson, 2001 p. 194; Humphrey and Konrad, 2000; van der Beek et al., 2002). This is less obvious in the case of small relative increases in elevation such as those in front of the Cangaime anticline (see, however, Bridge and Leeder, 1979; Alexander and Leeder, 1987; Dumont and Hanagarth, 1993) and this point will be discussed hereafter in each of the studied areas.

Styles of avulsions as defined by Slingerland and Smith characterize 3 different ways by which avulsions are achieved in the floodplain: (a) avulsion by annexation by which an existing channel is appropriated or reoccupied; (b) avulsion by incision, where new channels are scoured into the floodplain surface; and (c) avulsions by progradation, characterized by extensive deposition and multi-channeled distributive networks.

7.2.1- The avulsions in the MPA

The MPA represents an ancient megafan disconnected from the Pastaza system by a regional avulsion related to the propagation of the Cangaime thrust-fold. The high volume of sediment forming this megafan has been sufficient for the fan crest to constitute the divide between the Morona and Pastaza drainage basins until today, long after the abandon. In spite of the surimposition of the MCA

over its very apical part, the organisation of the megafan is well apparent in satellital images. As in other megafans having a moderate average slope such as the Kosi megafan in the Himalayan piedmont (Gole and Chitale, 1966; Wells and Dorr, 1987), large aggradation occurred and avulsions associating progradation and annexation predominate as suggested by the high amount of sediment distributed in the megafan and the multi-channeled distributive network. The switch of a channel into an adjacent one (which must not be confused with diverging/rejoining channels, see Wells and Dorr, 1987, fig. 2) can be interpreted as in the Kosi megafan (Wells and Dorr, 1987) as evidence of the lateral shifting of a single channel sweeping across the fan. Wells and Dorr (1987) interpreted the avulsions at the origin of the shifting of the Kosi River as results of overflow of both highly aggraded active rivers (alluvial ridges) and less aggraded pre-existing non-active or less active rivers in the inter-ridges areas, promoting drainage into the topographic lows at the cessation of flooding. No unusually large floods have been recorded in the upper Amazonian basin in the historical period which is probably more humid than the early Holocene when the MPA formed (see Weng et al., 2002). This constitutes a difference with the Kosi fan where huge floods have been recorded in the modern and recent times. In fact, Wells and Dorr (1987) demonstrated in the Kosi fan that major avulsions were not correlated with unusually high floods of any origin but were a result of 'normal' floods. However, 'normal' floods in the Kosi cover very large areas because of the very flat topography of the fan. The MPA fan is more bulged than the Kosi fan and the precipitation regime is not monsoonal. Therefore, wide annual floods are more difficult to invoke as triggers of avulsions in the MPA than in the Kosi system and the absence of wide annual floods like those occurring in the Kosi might explain the much lower frequency of avulsion in the MPA.

Other causes/triggers of avulsion in the MPA might be tectonics and volcanism. An influence of tectonics on avulsions is here rather unlikely because the MPA is relatively far from the active Subandean Frontal Trust and the Cutucu/Cangaime thrust-fold dome, and earthquakes recorded in the Amazonian domain are deep events with a relatively low magnitude.

The large-scale volcanic eruptions eventually capable of influencing the hydrologic regime of the Pastaza system when the MPA was active were a large rhyolitic eruption of the Cotopaxi, the first pyroclastic flows and associated lahars of the Chimborazo at 8000 – 5400 BC (Table), and the collapse of the Sangay II. Cotopaxi and Chimborazo volcanoes are far from the Amazonian domain and no traces of these events are found downstream of Baños in the western Eastern Cordillera (Bès de Berc et al., 2005). We have no information on the presence of products of the Sangay II collapse in, and downstream of, the terraces of the Rio Palora. The uncertainty of the date of this event (>14,000 years BP, Monzier et al., 1999) does not assure that it was contemporary with the construction of the MPA. Even though it were so, the along-stream distance between the MPA and the crater (~180 km) is very long when we consider than the 8 km^3 avalanche resulting from the 3000 years old collapse of the Tungarahua II travelled 'only' 21 km along the valley and that no traces of lahars following this event have been found in the Pastaza terraces near Mera at 60 km from the volcano (Bès de Berc et al., 2005). Therefore the Sangay II collapse could hardly have caused the abandon of the MPA megafan and it is unlikely that it might be a direct cause or trigger of the avulsions. However, the gradual erosion and transport in the fluvial system of the huge quantity of material provided by the volcanic eruptions coeval with, or older than, the MPA might have constituted a large part of thematerial accumulated in this area.

7.2.2 - The avulsions in the MCA

In the MCA the curved shape of the rivers shaping the propagation of Cangaime anticline and the avulsions only occurring in the downslope side of the rivers indicate that not only river migration but also avulsions have been controlled, at least in part, by tectonics. The local curved courses of rivers otherwise flowing south along the regional slope show that these rivers adapt locally to the new domal topography created by the propagation of the thrust-fold structure. The divergences at the origin of the successive paths, the clear separation between them, and the scarceness of meander mosaics (except locally in the west of path # 4 in Fig. 2) suggest that avulsion was there a more efficient process than progressive shifting to achieve this adaptation, even though progressive shifting may have locally occurred. At point A in Fig. 3, the avulsion from path #1 (Fig. 2) to path #2 (Fig.2) is clearly a result of the lateral propagation of the Cangaime fold defeating path #1 and transforming the water gap passing through the nose of the fold into a wind gap. In this case, fold growth is the major if not the unique cause of the avulsion (if a pure "mechanical" diversion like this one can be actually considered as a diversion). This is not the same for the other avulsions of the MCA. LANDSAT images of the streams affected by these avulsions indicate deposition along the valleys but the topographic sections normal to the rivers show V-shaped incised valleys with no evidence of levees or exhausted beds which could have shown that aggradation was the direct cause of avulsion. It might be objected that these V-shaped valleys have been incised by the rivers having reoccupied the abandoned valleys, but it is unlikely that the abandoned alluvial ridges would have been entirely removed as a result of incision by underfit streams. Therefore, even though the sedimentary/water discharges were probably as large as in the other parts of the Pastaza megafan complex, tectonic uplift resulting from the lateral/frontal propagation of the Cangaime thrust-fold seems here to have been the direct cause of the avulsions. This interpretation is also supported by the localization of the avulsions near the northern nose of this fold. Earthquakes such as the 1980 El Asnam (Algeria) earthquake (Philip and Meghraoui, 1983) capable of causing local rapid uplift of river beds could be possible triggers. Because of the absence of levees to be breached, seismic shaking alone as invoked by e.g. Stouthamer and Berendsen (2000) in the Rhine-Meuse delta, could hardly be taken as a possible trigger in the MCA in spite of markedly greater earthquake magnitudes. In contrast, intrinsic factors such as large floods may be considered as possible triggers even in this tectonically active context because aggradation may have elevated the river bed sufficiently for the flow to take advantage of the tectonic slope.

7.2.3 - The avulsions in the PCTB and the northern TCA.

In the TCA and the PCTB no field observations of avulsion features are available and satellite images only provide information on the size and arrangement of channels. However, the principal characteristic of these areas is the presence of diverted/rejoining channels forming anastomosing patterns still apparent in spite of vegetation growth. This suggests sustained avulsive flow transforming a floodplain into an avulsion belt showing abandoned anastomosed channels and small isolated flood basins as in the modern Saskatchewan River (Morozova and Smith, 2000; Slingerland and Smith, 2004) or other avulsion belts formed under various climatic regimes (e.g. Schumm et al., 1996; Smith et al., 1997; Bristow, 1999; Ethridge et al., 1999; and other refs in Slingerland and Smith, 2004). According to Slingerland and Smith's (2004) review, anastomosing reaches are results of progradational avulsions (Morozova and Smith, 2000) characterized by deposition out of the parent channel into the invaded floodplain and favoured by slow runoff promoted by low floodplain slopes (Slingerland and Smith, 2004, p. 264). The meandering streams occupying alluvial ridges such as the middle Rio Corrientes could be the new dominant meandering channel constituting the outcome of the evolution of the avulsion belt (fig. 2 in Slingerland and Smith, 2004). In most of the modern avulsion belts such the Saskatchewan River (Morozova and Smith, 2000), the Niobrara River (Ethridge et al., 1999), the Ovens and King rivers, Australia (Schumm et al., 1996) or the Brahmaputra River (Bristow, 1999), the causes of avulsions are entirely autocyclic and related to the high sedimentary discharge and deposition of these rivers even though the trigger was occasionally extrinsic (e.g. damming as for the Niobrara River, Ethridge et al., 1999). However, for Smith et al. (1997), neotectonic movement is the underlying cause of avulsion and anastomosis in the panhandle (upper entry corridor) of the Okavango fan situated in a 'relative' valley gradient depression inferred to represent a small graben. In the case of the PCTB and TCA, the avulsion belt is situated much too far from the active tectonic region, and the earthquake foci are too deep and their magnitude too low for tectonics to be the cause or trigger of the avulsions. For the same reasons as in the MPA, and notably the great distance to the volcanoes, volcanic eruptions, although frequent at the time when the PCTB and the MCA formed (see Table 1), cannot have been a direct cause or trigger of avulsion in these areas.

7.2.4 - The avulsions in the southern TCA and surrounding areas.

In the southern part of the TCA the fan shape is essentially apparent in the arrangement and shape of the numerous swamps of this region (Fig. 1). Well-characterized avulsions are rare. The style, cause, and triggers of avulsions seem to be researched in the very shallow attitude of the topography like in the 'losimean' megafans (Stanistreet and McCarthy, 1993) such as the Okavango (Stanistreet and Mc Carthy, 1993; Stanistreet et al., 1993) or the Taquari (Assine 2005; Assine and Soares 2004). In fact, the arrangement and shape of the swamps is likely to reflect the configuration of the floodplain and may be fed by temporary breaching of channel banks with short new channels being formed (Stanistreet et al., 1993). The predominance of low sinuosity channels is also a characteristic common to the southern TCA and the Okavango fan. We have no evidence in the southern TCA that channels are confined by vegetated and/or peat levees but no more evidence that they are not, and the similarity between the southern TCA and other very shallow humid fan such as the Okavango or the Taquari suggest that they might be.

7.3 - Remote causes of the avulsions in the Pastaza megafan complex

As discussed above, aggradation played a major role in the generation of avulsions in the different areas studied in the present paper, even in the MCA where tectonics prevails. This conclusion agrees with that of many authors having studied avulsions in various contexts, scale, and time lapses (see refs above). The origin of this large aggradation as a remote cause of avulsion is crucial in the Pastaza megafan complex where the catchment area (13,700 km^2) is much smaller than the depositional area (51,400 km^2). Table 2 shows characteristics of piedmont megafans in the Bolivian Andes (Rio Grande, Rio Pilcamayo, and Rio Parapeti, after Horton and DeCelles, 2001) and of the Kosi megafan compared with the Pastaza megafan complex. These characteristics include catchment and fan surfaces, fan/catchment ratio, water discharge, stream power per length unit, and incision rate. The entire Pastaza megafan complex has a much greater fan / catchment ratio (3.75 instead of 0.72 for the Rio Parapeti and 0.20-0.30 for the other systems). The contrast between the Pastaza megafan and the other megafans reduces if we consider only the MPA which is the first entity to have been formed and was abandoned when the eastern entities formed. If so, the fan / catchment ratio reduces to 1, which remains much higher than the other systems having similar stream powers per unit length. If we consider that the surface of the megafan is proportional to the volume of sediments preserved, then the volume of sediment transported per unit stream length was much greater for the Rio Pastaza than for the other systems presented in Table 2. Table 2 also shows that the Rio Parapeti which has a catchment surface close to that of the Rio Pastaza has a lower streampower and formed a much smaller fan, which would suggest that streampower is determinant in the construction of the fan. However, a comparison between the MPA and the Kosi indicate that the ratio of the catchment surfaces MPA / Kosi is 0.26 whereas the ratio of the fan surfaces MPA/Kosi is ~1.14. This means that the volume of material extracted from a unit surface might have been 4 times greater in the Pastaza catchment than in the Kosi catchment whereas the streampower of the Kosi River is twice that of the Pastaza. Now, if we compare the average values of incision rates for the Sun Kosi and Arun rivers (the junction of which gives birth to the Kosi river) in the Main Boundary Thrust – which are of 1.5 – 2.5 $mm.yr^{-1}$ (Lavé and Avouac 2001) – with those for the Pastaza in the Eastern Cordillera – which are of ~4 - 5 $mm.y^{-1}$ (Bès de Berc et al., 2005) – , it appears that the incision rates in the Pastaza are twice those in the Kosi. Because the streampower is twice lower in the Rio Pastaza than in the Kosi River, it is likely that the faster incision

rate in the Pastaza do reflect the rate of uplift of the Eastern Cordillera combined with a rapid adaptation of the river profile (Bès de Berc et al., 2005). Another cause must therefore be researched to the larger amount of material input into the Pastaza system.

In their study of tropical megafans, Leier et al. (2005) emphasized the contrast between the peak of discharge and the mean annual discharge, as a characteristic of all the megafans. The Rio Pastaza, like many other equatorial rivers (Latrubesse et al. 2007) does not display such a contrast in hydrologic cycles. Even during ENSO events, the ratio peak of discharge / mean annual discharge remain stable even though the mean annual discharge increases. Annual or episodic contrasts in hydrologic cycles are thus unable to explain the very large amount of sediment deposited by a fluvial system having a relatively small catchment. In any event, if this sediment were extracted by erosion from the bedrock of the catchment, this should imply a very rapid denudation and uplift of the entire Eastern Cordillera and eastern Western Cordillera of Ecuador during the late glacial period. The average denudation rate inferred by Vanacker et al. (2007) from their radionuclide studies in small basins of the eastern Cordillera is 0.2 mm $year^{-1}$. This value is considered to be high by these authors. However, such a denudation rate acting during the 11,000 yrs of activity of the MPA would have provided only ~30 km3 of material if we assume that the denudation rate was the same over the entire Pastaza basin (and less if the denudation rate was lower in the Interandean Depression as observed by Vanacker et al. (2007). Moreover, the uplift rate of4-5 mm/year uplift since the LGM observed by Bès de Berc et al. (2005) cannot be considered as a rapid uplift when values of ~2 cm/year have obtained in areas such as the Southern Alps of New Zealand). Volcanism may be another solution to this problem. As discussed above, it is unlikely that sedimentary pulses generated by volcanic eruption as previously proposed by Räsänen et al. (1990) were a direct cause or trigger of avulsions in any of the areas studied here. However, it is obvious that fluvial reworking of volcanic material associated to runoff and local landsliding in the easily erodable volcanic deposits has input volcanic material into the system. However, the estimate of the total volume of material provided by the volcanoes is of about 20 km^3 (see above). It should be pointed out that the addition of the material provided by the volcanic eruption and the denudation as inferred from the study of the cosmogenic radionuclides is only of ~50 km^3, which is small compared with the ~140 km3 of the MPA.. In any event, it is likely that the heavy volcano-sedimentary and sedimentary load transported down to the Amazonian lowland promoted aggradation and then avulsions as soon as the slope decreased. Even where the local cause or trigger of avulsion was not aggradation (e.g. the MCA) aggradation promoted by the heavy volcano-sedimentary load made the channel close to the avulsion threshold (Jones and Schumm, 1999) such that any 'opportunistic' event (Slingerland and Smith, 2004) can trigger avulsion. Conversely, aggradation may have triggered avulsion in areas such as the northern MCA where tectonic tilting has created a lateral slope more favourable to the avulsive channel but where the parent channel is confined by incised walls. In another ground, the prevalence of progradational avulsions in all the studied areas except the MCA could be taken as evidence that the high sedimentary load of the Pastaza system was the underlying cause of avulsion and and of the construction of very large megafans.

8 – Conclusions

Remote sensing imagery mapping of the successive channels of the Rio Pastaza enabled us to evidence 108 sites of avulsion in the Rio Pastaza megafan. The location of these sites, the available radiocarbon ages as well as historic maps of the 17th century, allow us to propose an evolution of the migration and avulsions of the Rio Pastaza since the Last Glacial Maximum.

The first avulsions of the Rio Pastaza occurred after the LGM roughly parallel to the Subandean front and gave rise to a well defined fan-shaped distributary pattern (Fig. 9A). In response to thrust-related anticline forelimb tilt, the Rio Pastaza and the apex of the megafan were progressively shifted eastward until the "Great Diversion" of the Rio Pastaza changed its course to the east-southeast towards the present-day Rios Tigre and Corrientes (TCA) (Fig.9B). Around 9200±200 or 8480±110 Cal years BP, avulsions occurred in the TCA (Fig.9C). The Rio Pastaza abandoned then its east-southeast course and the Tigre-Corrientes area to follow its present-day southerly course. This last avulsion was older than 1691AD (Fig. 9D).

The average recurrence time of avulsions in the Marañon-Pastaza area, probably overestimated, ranges between 142±6 years and 189±6years whereas in the Tigre-Corrientes areas, the average recurrence time of avulsions is underestimated and ranges from 342±5years to 426±10years.

Regional tectonics is active in the northwest of the Maranon-Pastaza area and responsible for thrust-related anticline eastward forelimb tilt and lateral propagation is believed to have controlled most of the avulsions in this area. No such tectonic control seems to have acted in the south of the MPA and the TCA. The characteristics of the hydrologic cycles of the Rio Pastaza doe not allow "hydrologic" driven avulsions such as those known in areas characterized by contrasted hydrologic cycles invoked by Leier et al. (2005) in other megafans. Climatic fluctuations or pulses in sedimentary fluxes, not clearly related to volcanic activity as previously proposed by Räsänen et al. (1990), seem to be the most likely cause of avulsions in those areas.

Acknowledgements

This study benefited of the logistic and financial support of the IRD (French Institute for Research in Development). This investigation was supported by a doctoral Alban fellowship (n° E05D057404EC) and Université Toulouse III, Paul Sabatier grants.

REFERENCES

Alexander J and Leeder MR, 1987. Active tectonic control of alluvial architecture. In: F.G. Ethridge, R.M. Flores and M.D. Harvey (Eds.), Recent developments in fluvial sedimentology. Special Publication. SEPM (Society for Sedimentary Geology), pp. 243-252.

Assine ML, 2005. River avulsions on the Taquari megafan, Pantanal wetland, Brazil. Geomorphology, 70: 357-371.

Assine ML and Soares PC, 2004. Quaternary of the Pantanal, west-central Brazil. Quaternary International, 114: 23-34.

Autin WJ, Burns SF, Miller BJ, Saucier RT and Snead JL, 1991. Quaternary Geology of the Lower Mississipi Valley. In: R.B.

Morrison (Ed.), Quaternary Nonglacial Geology: Conterminous U.S. Geology of North America. Geological Society of America, pp. 547-582.

Baby P, Rivadeneira M, Christophoul F and Barragán R, 1999. Style and timing of deformation in the Oriente of Ecuador. In: Orstom (Ed.), 4th International Symposium of Andean Geodynamics. ORSTOM, Göttingen, pp. 68-72.

Barba D, Robin C, Samaniego P and Eissen J-P, 2008. Holocene recurrent explosive activity at chimborazo volcano (Ecuador). Journal of Volcanology and Geothermal Research, 176: 27-35.

Barberi F, Coltelli M, Ferrara G, Innocenti F, Navarro, J-M, Santacroce R, 1988. Plio-Quaternary volcanism in Ecuador. Geological Magazine, 125(1): 1-14.

Baret F and Guyot G, 1991. Potentials and limits of vegetation indices for LAI and APAR assessment. Remote Sensing of Environment, 35(161–173).

Barragann R, Baudino R and Marocco R, 1996. Geodynamic evolution of the Neogene intermontane Chota basin, Northern Andes of Ecuador. Journal of South American Earth Sciences, 9(5-6): 309-319.

Behling H and Hooghiemstra H, 1999. Environmental history of the Colombian savannas of the Llanos Orientales since the last glacial maximum from lake records El Pinal and Carimagua. Journal of Paleolimnology, 21: 461–476.

Behling H and Hooghiemstra H, 1998. Late quaternary palaeoecology and palaeoclimatology from pollen records of the savannas of the Llanos Orientales in Colombia. Palaeogeography Palaeoclimatology Palaeoecology, 139: 251– 265.

Bes de Berc S, Soula J-C, Baby P, Souris M, Christophoul F and Rosero M, 2005. Geomorphic evidence of active deformation and uplift in a modern continental wedge-top - foredeep transition: example of the eastern Ecuadorian Andes. Tectonophysics, 399(1-4): 351-380.

Blair TC and McPherson JG, 1992. The Trolheim fan and facies model revisited. Geological Society of America Bulletin, 104(6): 762-769.

Bourdon E, Eissen J-P, Gutscher MA, Monzier M, Hall ML, Cotten J, 2003. Magmatic response to early aseismic ridge subduction: the Ecuadorian margin case (South America). Earth and Planetary Science Letters, 3205(3-4): 123-138.

Bridge JS and Karssenberg D, 2005. Simulation of flow and sedimentary processes, including channel bifurcation and avulsion, on alluvial fans., 8th International Conference of Fluvial Sedimentology, TU Delft, Netherlands, pp. 70.

Bridge JS and Leeder MR, 1979. A simulation model of alluvial stratigraphy. Sedimentology, 26: 617-634.

Bristow CS, 1999. Gradual avulsion, river metamorphosis and reworking by underfitd streams: a modern example from the Brahmaputra river in Bangladesh and a possible ancient example in the Spanish Pyrenees. In: N.D. Smith and J. Rogers (Eds.), Fluvial Sedimentology VI. Special Publication of the International Association of Sedimentologists #28, pp. 221-230.

Burbank DW and Anderson RS, 2001. Tectonic Geomorphology. Blackwell Science, 274 pp.

Burbank DW, 1996. Causes of the recent Himalayan uplift deduced from deposited pattern in the Ganges Basin. Nature, 357: 680-682.

Burgos JD, 2006. Mise en place et progradation d'un cône alluvial au front d'une chaîne active: exemple des Andes équatoriennes au néogène. Phd Thesis, Université Paul Sabatier, Toulouse 3, Toulouse, 373 pp.

Castro M, Mothes P, Hidalgo J, Samaniego P, Hall ML, Galarraga R, Yepes H, Andrade D, Ruiz AG, 2006, Recent numerical modeling of Cotopaxi's lahars, Ecuador, Abstract Cities on Volcanoes 4, Quito, 23-27 January 2006.

Catuneanu O, 2004. Retroarc foreland systems - Evolution through times. Journal of African Earth Sciences, 38: 225-242.

Christophoul F, Baby P, Soula J-C, Rosero M and Burgos JD, 2002. Les ensembles fluviatiles néogènes du bassin subandin d'Equateur et implications dynamiques. Compte Rendus Géosciences, 334: 1029-1037.

Clapperton CM, Hall M, Mothes P, Hole MJ, Still JW, Helmens KF, Kuhry P, Gemmel AMD, 1997. A younger dryas icecap in the Ecuadorian Andes. Quaternry Research, 47: 13– 28.

Cobb KM, Charles CD, Cheng H and Edwards RL, 2003. El Niño Southern Oscillation and tropical Pacific climate during the last millenium. Nature, 424: 271– 276.

DeCelles PG and Giles KA, 1996. Foreland Basin Systems. Basin Research, 8: 105-123.

Demoraes F and d'Ercole R, 2001. Cartografıa de riesgos y capacidades en el Ecuador. Diagnostico previo a planes de intervencion de las ONGs, International report. COOPI-IRD-OXFAM, Quito (Ecuador).

Dumont J-F, 1996. Neotectonics of the Subandes-Brazilian craton boundary using geomorphological data: the Marañon and Beni Basin. Tectonophysics, 257: 137-151.

Dumont JF and Hanagarth W, 1993., 1993. River shifting and tectonics in the Beni Basin (Bolivia), Proceedings of the 3rd International Conference of Geomorphology, 23-29 August, Hamilton, ON.

Eguez A, Alvarado A, Yepes H, Machette MN, Costa C, Dart RL, Bradley LA, 2003. Database and Map of Quaternary Faults and Folds of Ecuador and its offshore regions. USGS Open-File Report, 03-289, 71 pp.

Ethridge FG, Skelly RL and Bristow CS, 1999. avulsion and crevassing in the sandy, braided Niobrara River: complex response to base-level rise and aggradation. In: N.D. Smith and J. Rogers (Eds.), Fluvial Sedimentology VI. Special Publication of the International Association of Sedimentologists #28, pp. 180-191.

Fauchet B and Savoyat E, 1973. Esquisse Géologique des Andes de l'Equateur. Revue de Géographie Physique et de Géologie Dynamique, XV(1-2): 115-142.

Friend PF, Jones NE and Vincent SJ. 1999. drainage evolution in active mountain belts: extrapolation backwards from present-day Himalayan river pattern. In: N.D. Smith and J. Rogers (Eds.), Fluvial Sedimentology VI. Special Publication #28 of the International Association of Sedimentologists. Blackwell, pp. 305-313.

Frost I, 1998. A Holocene sedimentary record from Añangucocha in the Ecuadorian Amazon. Ecology, 69: 66– 73.

Gohain K and Parkash B, 1990. Morphology of the Kosi Megafan. In: AH Rachoki and M Church (Eds.), Alluvial Fans: a field approach. Wiley, pp. 151-178.

Gole CV and Chitale SV, 1966. Inland delta building activity of Kosi River. American Society of Civil Engeneers Journal, Hydraulic Division, HY-2: 111-126.

Gomez N, 1994. Atlas del Ecuador, Geografia y Economia. Imagenes de la Tierra, 3. Editorial Ediguias C. Ltda., Quito, 114 pp.

Guth PL, 2006, Geomorphometry from SRTM: Comparison to NED: Photogrammetric Engineering & Remote Sensing, 72(3),269-277.

Haberle S, 1997. Late Quaternary vegetation and climate history of the Amazon basin: correlating marine and terrestrial pollen records. Proceedings of the Ocean Drilling Project, Scientific results, 155: 381–396.

Hall M and Beate B, 1991. El volcanismo Plio-Cuaternario en los Andes del Ecuador. Estudios Geograficos, 4: 5– 38.

Hall ML, 1977. El volcanismo en el Ecuador. Publicacion del Instituto Panamericano de Geografia e Historıa, Seccion Nacional del Ecuador., Quito, 120 pp.

Hall, ML, (coord), 1991, The March 5, 1987 Ecuador Earthquake, Mass wasting and socioeconomic effects, The national academic Press, Washington DC, 144pp.

Hall ML, Samaniego P, LePennec J-L and Johnson JB, 2008. Ecuadorian Andes volcanism: A review of Late Pliocene to present activity. Journal of Volcanology and Geothermal Research, 171: 1-6.

Hall ML, Robin C, Beate B, Mothes P and Monzier M, 1999. Tungurahua Volcano, Ecuador: structure, eruptive history and hazards. Journal of Volcanology and Geothermal Research, 91(1): 1-21.

Hansen BCS, Rodbell DT, Seltzer GO, Leon B, young K.R. and Abbott M, 2003. Late-glacial and Holocene vegetational history from two sites in the western Cordillera of southwestern Ecuador. Palaeogeography Palaeoclimatology Palaeoecology, 194: 79–108.

Hastenrath S and Kutzbach J, 1985. Late Pleistocene climate and water budget of the South American Altiplano. Quaternary Research, 24: 249–256.

Hastenrath S, 1981. The glaciation of the Ecuadorian Andes. Balkema, Rotterdam.

Heine K, 2000. Tropical South America during the Last Glacial Maximum: evidence from glacial, peri-glacial and fluvial records. Quaternary International, 72: 7-21.

Heine K and Heine JT, 1996. Late glacial climatic fluctuations in Ecuador. Glacier retreat during the Younger Dryas time. Arctic and Alpine Research, 28: 496-501.

Heine K, 1994. The Mera site revisited: Ice-age Amazon in the light of new evidence. Quaternary International, 21: 113-119.

Hooghiemstra H and Van Der Hammen T, 1998. Neogene and Quaternary development of the neotropical rain forest: the forest refugia hypothesis, and a literature overview. Earth Science Review, 44(3-4): 147-183.

Horton BK and DeCelles PG, 2001. Modern and ancient fluvial megafans in the foreland basin system of the Central Andes, Southern Bolivia: implications for drainage network evolution of fold-thrust belts. Basin Research, 13: 43-63.

Humphrey NF and Konrad SK, 2000. River incision or diversion in response to bedrock uplift. Geology, 28: 43-46.

Hungerbühler D, Steinman M, Winkler W, Seward D, Egüez A, Peterson DE, Helg U, Hammer C, 2002. Neogene stratigraphy and Andean geodynamics of southern Ecuador. Earth Science Review, 57: 75–124.

IGEPN, 2009. http://www.igepn.edu.ec, Instituto Geofisico de la Escuela Politecnica Nacional, Quito, ecuador.

Jones LS and Schumm SA, 1999. Causes of avulsion: an overview. In: ND Smith and J Rogers (Eds.), Fluvial Sedimentology VI. Special Publication of the International Association of Sedimentologists. Blackwell Science, pp. 171-178.

Jones LS and Harper JT, 1998. Channel avulsions and related processes, and large scle sedimentation patterns since 1875, Rio Grande, San Luis Valley, Colorado. Geological Society of America Bulletin, 110(3): 411-421.

Keefer DK, Moseley ME and deFrance S, 2003. A 38000-year record of floods and debris flows in the Ilo region of southern Peru and its relation to El Niño events and great earthquakes. Palaeogeography Palaeoclimatology Palaeoecology, 194: 41– 77.

Kennerley JB, 1980. Outline of the Geology of Ecuador. Overseas Geological and Mineral Resources, 55: 1-16.

Lang HR, and Welch R, (1994), « Algorithm Theoretical Basis Document for ASTER Digital Elevation Models: », Jet Propulsion Laboratory, May 31, 1994, draft report to the EOS Project.

Latrubesse, E.M., Stevaux, J.C. and Sinha, R., 2007. Tropical Rivers. Geomorphology, 70(3-4): 187-206.

Lavé J and Avouac J-P, 2001. Fluvial incision and tectonic uplift across the Himalaya of Central Nepal. Journal od Geophysical Research, 106(B11): 26,561-26,591.

Lavenu A, Noblet C, Bonhomme MG, Egüez A, Dugas F, Vivier G, 1992. New K-Ar age dates of Neogene and Quaternary volcanic rocks from the Ecuadorian Andes: Implications for the relationship between sedimentation, volcanism, and tectonics. Journal of South American Earth Sciences, 5(3-4): 309-320.

Ledru M-P, Bertaux J, Sifeddine A and Suguio K, 1998. Absence of last glacial maximum records in lowland tropical forests. Quaternary Research, 49: 233– 237.

Leeder MR, Harris T and Kirby MJ, 1998. Sediment supply and climate change: implications for basin stratigraphy. Basin Research, 10: 7 – 18.

Legrand D, Baby P, Bondoux F, Dorbath C, Bes de Berc S, Rivadeneira M, 2005. The 1999-2000 seismic experiment of Macas swarm (Ecuador) in relation with rift inversion in subandean foothills. Tectonophysics, 395: 67-80.

Leier AL, DeCelles PG and Pelletier JD, 2005. Mountains, Monsoons and megafan. Geology, 33(4): 289-292.

LePennec J-L, Jaya D, Samaniego P, Ramon P, Moreno Yanez S, Egred J, Van der Plicht J 2008. the AD1300-1700 eruptive periods et Tungurahua vocano, Ecuador, revealed by historical narratives, stratigraphy and radiocarbon dating. Journal of Volcanology and Geothermal Research, 176: 70-81.

Li S and Finlayson B, 1993. Flood management on the lower Yellow River: hydrological and geomorphological perspectives. In: C.R. Fielding (Ed.), Current Research in Fluvial Sedimentology. Sedimentary Geology, 85, pp. 285-296.

Mackey SD and Bridge JS, 1995. Three dimensional model of alluvial stratigraphy: Theory and application. Journal of Sedimentary Research, B65(1): 7-31.

Makaske B, 2001. Anastomosing rivers: a review of their classification, origin and sedimentary products. Earth Science Review, 53: 149-196.

McClay KR, 1992. Glossary of thrust tectonics. In: K.R. McClay (Ed.), Thrust Tectonics. Chapman and Hall, London, pp. 447.

Mégard F, 1984. The Andean Orogenic Period and its Major Structures in Central and Northern Peru. Journal of the Geological Society of London, 141: 893-900.

Montufar R and Pintaud J-C, 2006. Variation in species composition, abundance and microhabitat preferences among western Amazonian Terra Firme palm communities. Botanical Journal of the Linnean Society, 151: 127-140.

Monzier M, Robin C, Samaniego P, Hall ML, Cotten J, Mothes P, Arnaud N, 1999. Sangay volcano, Ecuador: structural development, present activity and petrology. Journal of Volcanology and Geothermal Research, 90(1-2): 49-79.

Morozova GS and Smith ND, 2000. Holocene avulsion styles and sedimentation patterns of the Saskatchewan River, Cumberland Marshes, Canada. Sedimentary Geology, 130: 81-105.

Morozova GS and Smith ND, 1999. Holocene avulsion history of the lower Saskatchewan fluvial system, Cumberland Marshes, Saskatchewan-Manitoba, Canada. In: N.D. Smith and J. Rogers (Eds.), Fluvial Sedimentology VI. Special Publication. International Association of Sedimentologists, pp. 231-249.

Moy CM, Seltzer GO, Rodbell DT, Anderson DM, 2002. Variability of El Niño/Southern Oscillation activity at millennial timescales during the Holocene epoch. Nature, 420, pp. 162- 165.

Nelson BW, 1970. Hydrography, sediment dispersal and recent historical development of the Po River Delta, Italy. In: J.P. Morgan and R.H. Shaver (Eds.), Deltaic Sedimentation, Modern and Ancient. Special Publication. SEPM, pp. 152-184.

Philip H and Meghraoui M, 1983. Structural analysis and interpretation of the surface deformation of the El Asnam earthquake of October 10, 1980. Tectonics, 2(1): 17-49.

Potts LV, Akyilmaz O, Braun A, Shum CK, 2008. Multi-resolution dune morphology using Shuttle Radar Topography Mission (SRTM) and dune mobility from fuzzy inference systems using SRTM and altimetric data, International Journal of Remote Sensing, 29 , 2879-2901.

Pratt WR, Duque P and Ponce M, 2005. An autochthonous geological model for the eastern Andes of Ecuador. Tectonophysics, 399(1-4): 251-278.

Ramsay J, 1967. Folding and fracturing of rocks. MacGraw-Hill, New York, 568 pp.

Ramsay JG and Huber MI, 1987. The techniques of modern structural geology, vol2: Folds and Fractures. Academic Press, 307 pp.

Räsänen ME and Linna AM, 1996. Miocene deposits in the Amazonian Foreland Basin. Science, 273: 124, 125.

Räsänen ME, Neller R, Salo J and Jungner H, 1992. Recent and ancient fluvial deposition systems in the Amazonian foreland basin, Peru. Geological Magazine, 129: 293-306.

Räsänen ME, Salo JS, Jungnert H and Romero Pittman L, 1990. Evolution of the Western Amazon Lowland Relief: Impact of Andean Foreland Dynamics. Terra Nova, 2: 320-332.

Reimer PJ, Baillie MGL, Bard E, Bayliss A, Beck JW, Bertrand CJH, Blackwell PG, Buck CE, Burr GS, Cutler KB, Damon PE, Edwards RL, Fairbanks RG, Friedrich M, Guilderson TP, Hogg G, Hughen KA, Kromer B, McCormac G, Manning S, Ramsey CB, Reimer RW, Remmele S, Southon JR, Stuiver M, Talamo S, Taylor FW, Van der Plicht J, Weyhenmeyer CE, 2004. INTCAL04 Terrestrial Radiocarbon age calibration, 0-26 Cal kyrs BP. Radiocarbon, 46(3): 1029-1058.

Reynaud C, Jaillard E, Lapierre H, Mamberti M and Mascles G, 1999. Oceanic plateau and island arcs of southwestern Ecuador: their place in the geodynamic evolution of northwestern South America. Tectonophysics, 307: 235-254.

Rodbell DT, Seltzer GO, Anderson DM, Abbott MB, Enfield DB, Newman JH, 1999. A high resolution ~15,000 record of El-Nino driven alluviation in southwestern Ecuador. Science, 283: 516-519.

Roddaz M, Baby P, Brusset S, Hermoza W and Darrozes J, 2005. Forebulge dynamics and environmental control in Western Amazonia: The case study of the Arch of Iquitos (Peru). tectonophysics, 399(1-4): 87-108.

Rosseti D and Valeriano MM, 2007. Evolution of the lowest amazon basin modeled from the integration of geological and SRTM topographic data. Catena, 70: 253-265.

Saucier RT, 1994. Geomorphology and Quaternary geologic history of the Lower Mississipi Valley. U.S. Army Corps of Engineers, 1: 1-364.

Schumm SA, Dumont J-F and Holbrook JM, 2000. active tectonics and alluvial rivers. Cambridge University Press, 276 pp.

Schumm SA, Erskine WD and Tilleard JW, 1996. Morphology, hydrology, and evolution of the anastomosing Ovens and King Rivers, Victoria, australia. Geological Society of America Bulletin, 108(10): 1212-1224.

Schumm SA, Mosley MP and Weaver WE, 1987. Experimental Fluvial Geomorphology. Wiley Interscience, New York, 411 pp.

Seltzer GO, Rodbell PA, Baker SC, Fritz PM, Tapia HD, Rowe RB, Dunbar RB, 2002. Early warming of Tropical South America at the last glacial transition. Science, 296: 1685-1686.

Singh IB, Parkash B and Gohain K, 1993. Facies anlysis of the Kosi Megafan deposits. Sedimentary Geology, 85(87-113).

Slingerland R and Smith ND, 2004. River avulsion and their deposits. Annual Reviews of Earth and Planetary Science, 32: 257-285.

Smith ND, McCarthy TS, Ellery WN, Merry CL and Ruther H, 1997. Avulsion and anastomosis in the panhandle region of the Okavongo Fan, Botswana. Geomorphology, 20: 49-65.

Spikings RA, Seward D, Winkler W and Ruiz G, 2000. Low temperature thermochronology of the northern Cordillera Real, Ecuador: tectonic insights from zircon and apatite fission track analysis. Tectonics, 19: 648– 649.

Spikings RA and Crowhurst PV, 2004. (U/Th)He thermochronometric constraints on the late Miocene Pliocene development of the northern Cordillera Real and Interandean Depression. Journal of South American Earth Sciences.17:239-251.

Stanistreet IG, Cairncross B and McCarthy TS, 1993. Low sinuosity and meandering bedload rivers of the Okavango Fan: channel confinement by vegetated levees without fine sediment. Sedimentary Geology, 85 (1–4): 135-156.

Stanistreet IG and McCarthy TS, 1993. The Okavango Fan and the classification of subaerial fan systems. Sedimentary Geology, 85: 115-133.

Stinton, A.J., and Sheridan, M.F., 2008, Implications of long-term changes in valley geomorphology on the behavior of small-volume pyroclastic flows, J. Volcanology and Geothermal Research. 176, 134-140,

Stouthamer E and Berendsen HJA, 2001. Avulsion Frequency, Avulsion duration and interavulsion period of the Holocene channel belts in the Rhine-Meuse Delta, The Netherlands. Journal of Sedimentary Research, 71(4): 589-598.

Stouthamer E and Berendsen HJA, 2000. Factors Controlling the Holocene Avulsion History of the Rhine-Meuse Delta (The Netherlands). Journal of Sedimentary Research, 70(5): 1051-1064.

Talling PJ and Sowter MJ, 1998. Erosion, deposition and basin wide variations in stream power and bed shear stress. Basin Research, 10: 87-108.

Törnqvist TE and Bridge JS, 2002. Spatial variation of overbank aggradation rates and its influence on avulsion frequency. Sedimentology, 49: 891-905.

Törnqvist TE, 1994. Middle and late Holocene avulsion history of the River Rhine (Rhine-Meuse Delta, Netherlands). Geology, 22: 711-714.

Tschopp HJ, 1953. Oil explorations in the Oriente of Ecuador. American Association of Petroleum Geologists Bulletin, 37: 2303-2347.

Vanacker V, von Blanckenburg F, Govers G, Kubik PW, 2007. Transient landscape evolution following uplift in the Southern Ecuadorian Andes, Geochimica and Cosmogenica Acta, 71: A1052.

Vanacker V, von Blanckenburg F, Govers G, Molina A, Poesen J, Deckers J, Kubik P.W, 2007. Restoring natural vegetation reverts mountain erosion to natural levels, Geology, 35: 303-306.

van der Beek P, Champel B and Mugnier J-L, 2002. Control of detachment dip on drainage development in regions of active fault-propagation folding. Geology, 30(5): 471-474.

Welch R and Marko W, (1981), « Cartographic potential of spacecraft line-array camera system: », Stereosat, Photogrammetric Engineering and Remote Sensing, v. 47, n. 8, p.1173-1185.

Weng C, Bush MB, Athens JS, 2002. Holocene climate changeand hydrach succession in lowland Amazonian Ecuador. Review of Palaeobotany and Palynologt 120, 73– 90.

Wells NA and Dorr JA, 1987. Shifting of the Kosi River, Northern India. Geology, 15: 204-207.

Winkler W, Villagomez D, Spikings R, Abegglend P, Toblere S and Egüez A, 2005. The Chota basin and its significance for the inception and tectonic setting of the inter-Andean depression in Ecuador. Journal of South American Earth Sciences, 19(1): 5-19.

Zandbergen P, 2008, Applications of Shuttle Radar Topography Mission Elevation Data, Geography Compass, Earth observation, DOI: 10.1111/j.1749-8198.2008.00154.x.

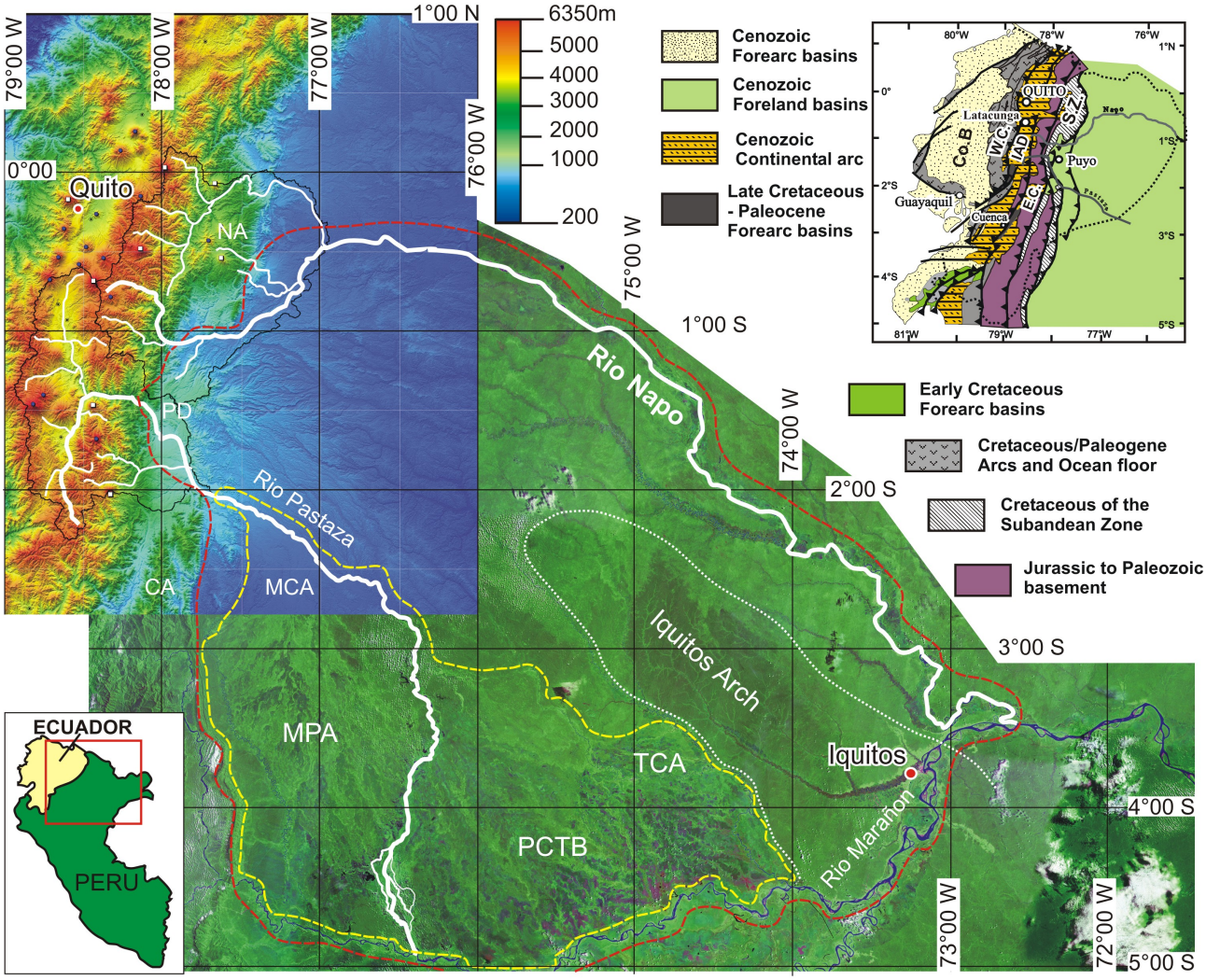

Figure 1 : Composite map of the Napo-Pastaza Megafan (DEM SRTM 3" resolution and Landsat 7). Solid black lines: limits of the Napo and Pastaza catchments, solid white lines: modern Rio Napo and Pastaza, red dashed lines: limits of the Plio-Pleistocene Napo Pastaza Megafan, yellow dashed lines: post-LGM Pastaza Megafan. Blue points: volcanoes, white squares: actives volcanoes. NA: Napo Antiform, PD: Pastaza Depression, CA: Cutucu Antiform, MCA: Morona Cangaime Area, MPA: Morona Pastaza Area, TCA, Tigre Corrientes Area, PCTB: Pastaza Corrientes Transition Band.

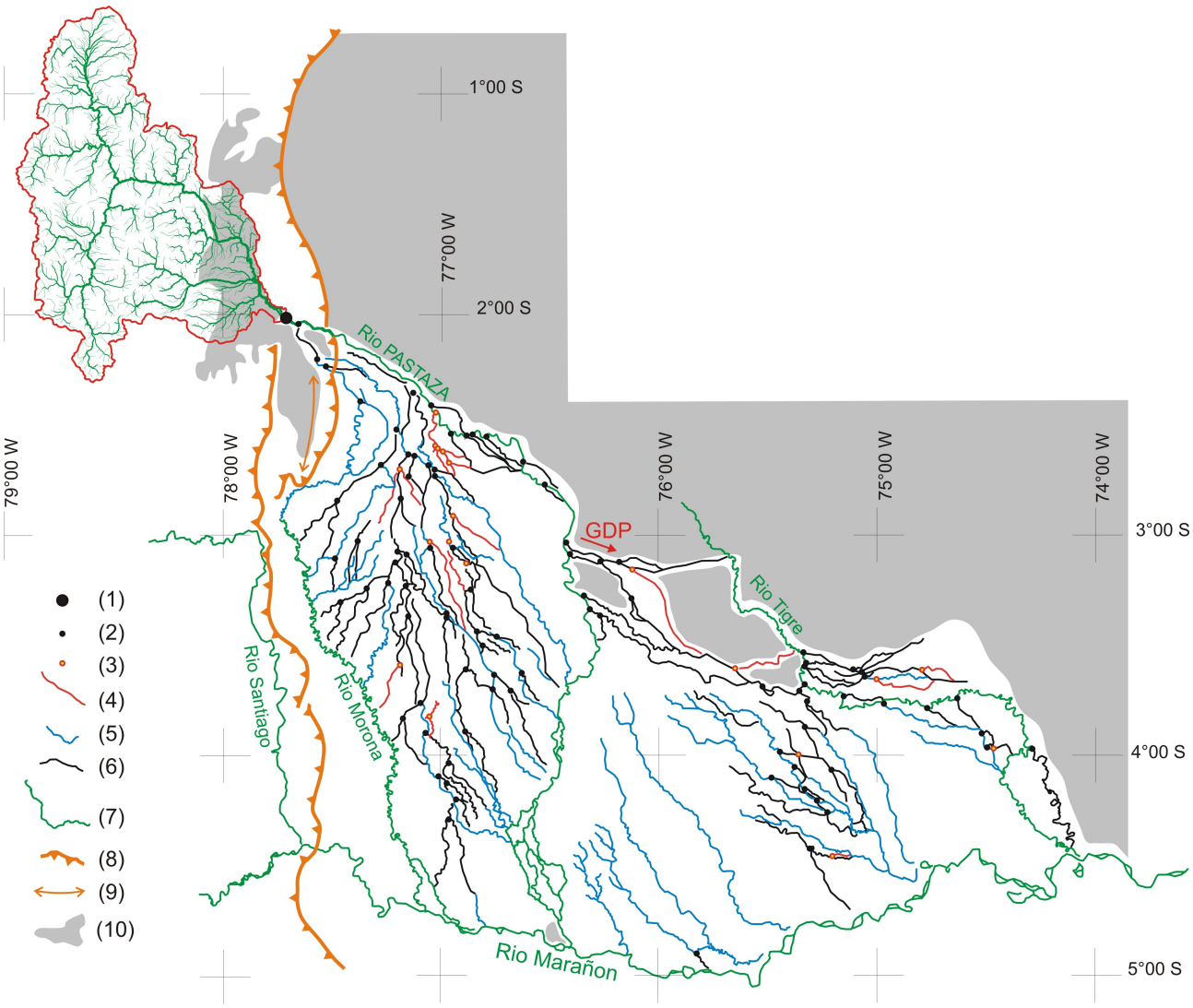

Figure 2 : Hydrographic network of the Rio Pastaza basin. To the northwest, with red lines: catchment of the Rio Pastaza Megafan (extracted from the SRTM DEM). With green lines: drainage network. Thickness of lines depends on the Stralher order of the streams. Thinnest lines correspond to Order 3 streams. 1) Modern apex of the Pastaza Megafan, 2) avulsion sites, 3) supposed avulsion sites, 4) abandoned stream, 5) abandoned stream re-annexed by the modern drainage network, 6) supposed abandoned stream, 7) main modern streams, 8) eastern boundary of the subandean tectonic structures, 9) Cangaime anticline axis.

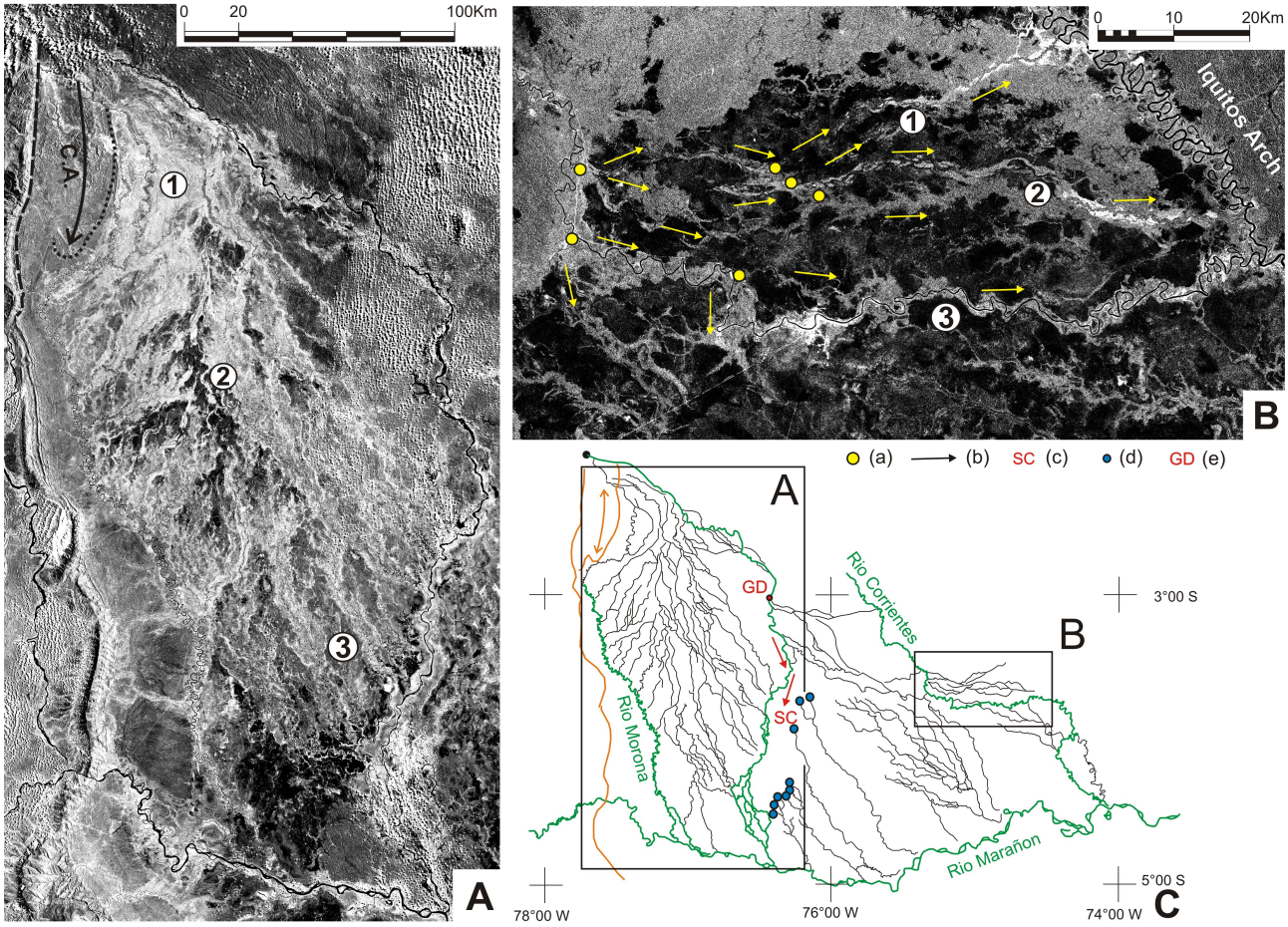

Figure 3: Examples of successives courses and avulsion sites of the Rio Pastaza. A) Morona Pastaza area (MPA), C.A. : Axis of the Cangaime anticline, 1,2 and 3, see text for explanation. B) Northern part of the area of the Rio Tigre and Corrientes (TCA), (a) avulsion sites, (b) plaeocurrents in abandoned reaches, 1, 2 and 3, see text for explanation. C) Location map of images A and B within the pastaza megafan. (c) Southern Curve of the Rio Pastaza resulting from the last signficative avulsion of the Rio Pastaza (prior to 1691AD), (d) Streams beheaded as a consequence of the avulsion which gave birth to SC, (e) GDP: avulsion site of the Great Diversion of the Rio Pastaza by mean of which the Rio Pastaza passed from the MPA to the TCA. Image Landsat 7.

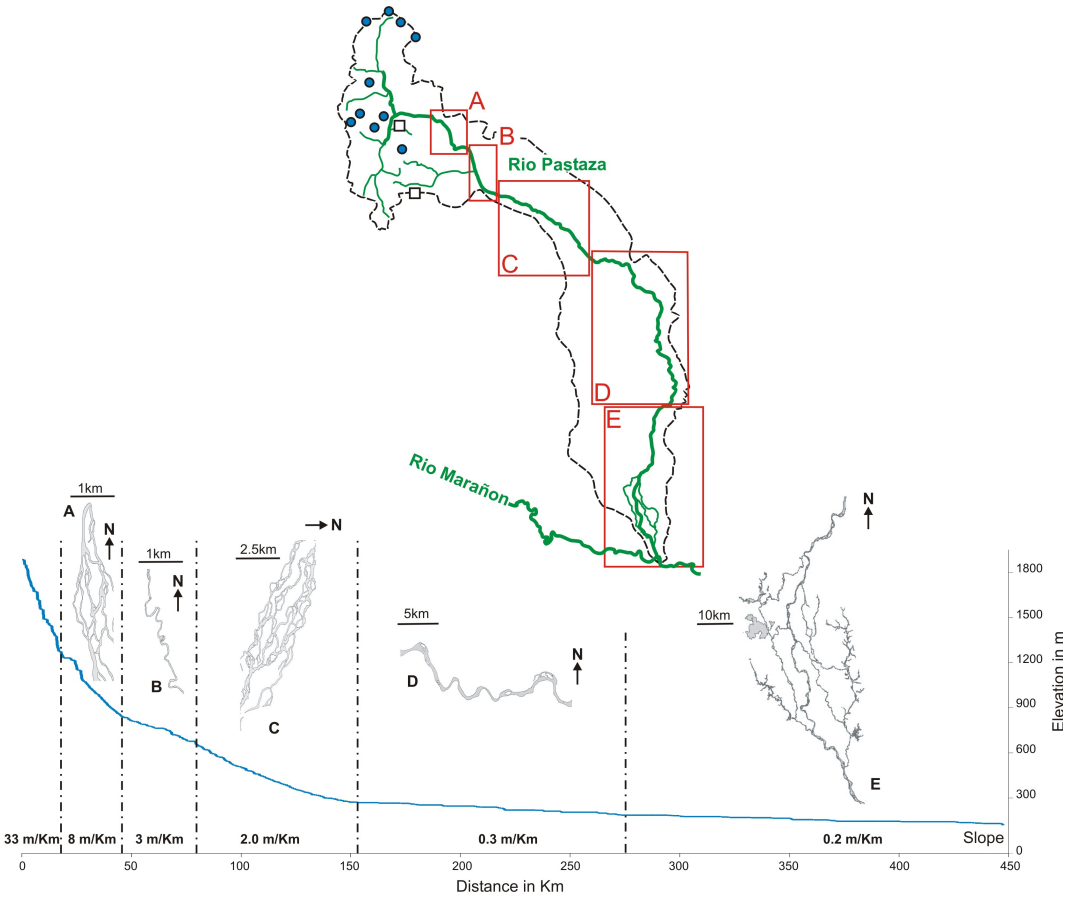

Figure 4 : Schematic map of the Rio Pastaza drainage basin, river profile, slope and associated channel pattern of the Rio Pastaza (profile extracted from the SRTM V3 DEM of the area)

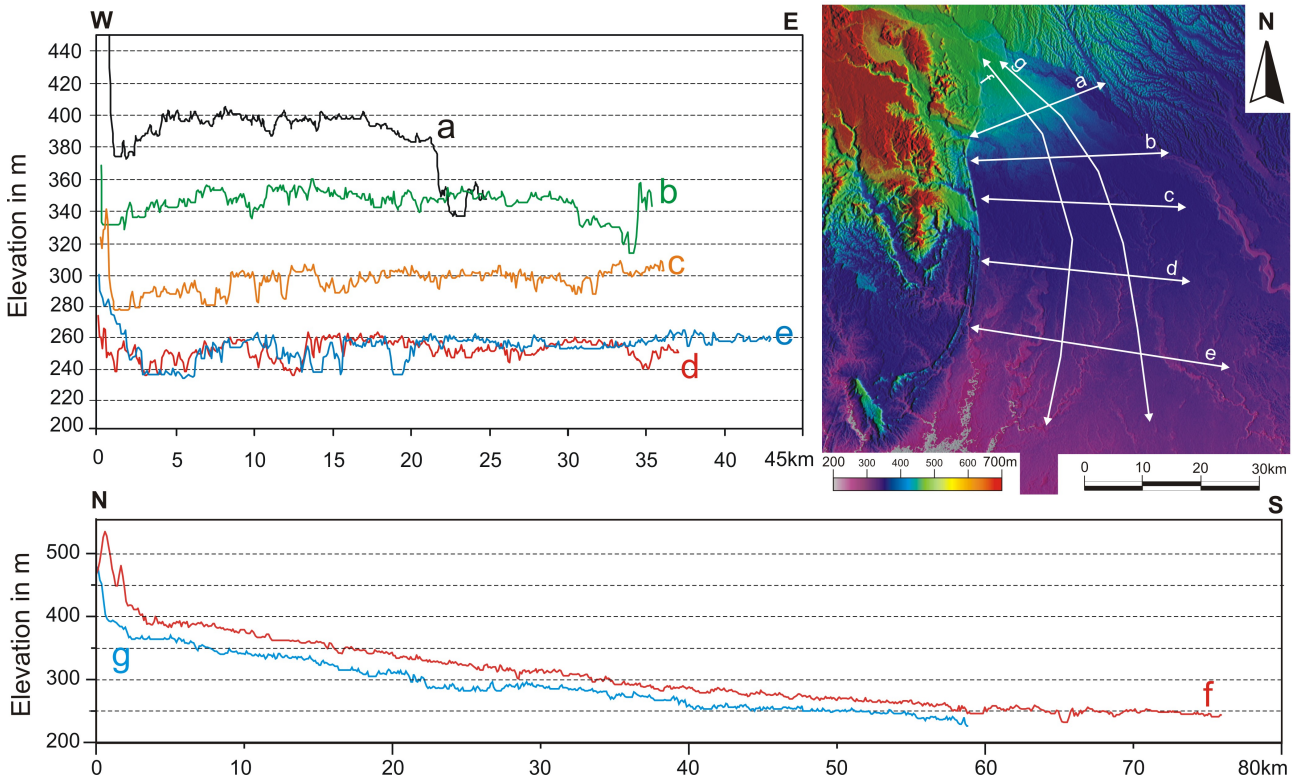

Figure 5: Topographic profiles extracted from the SRTM DEM showing the topography of the upper part of the Pastaza Megafan.

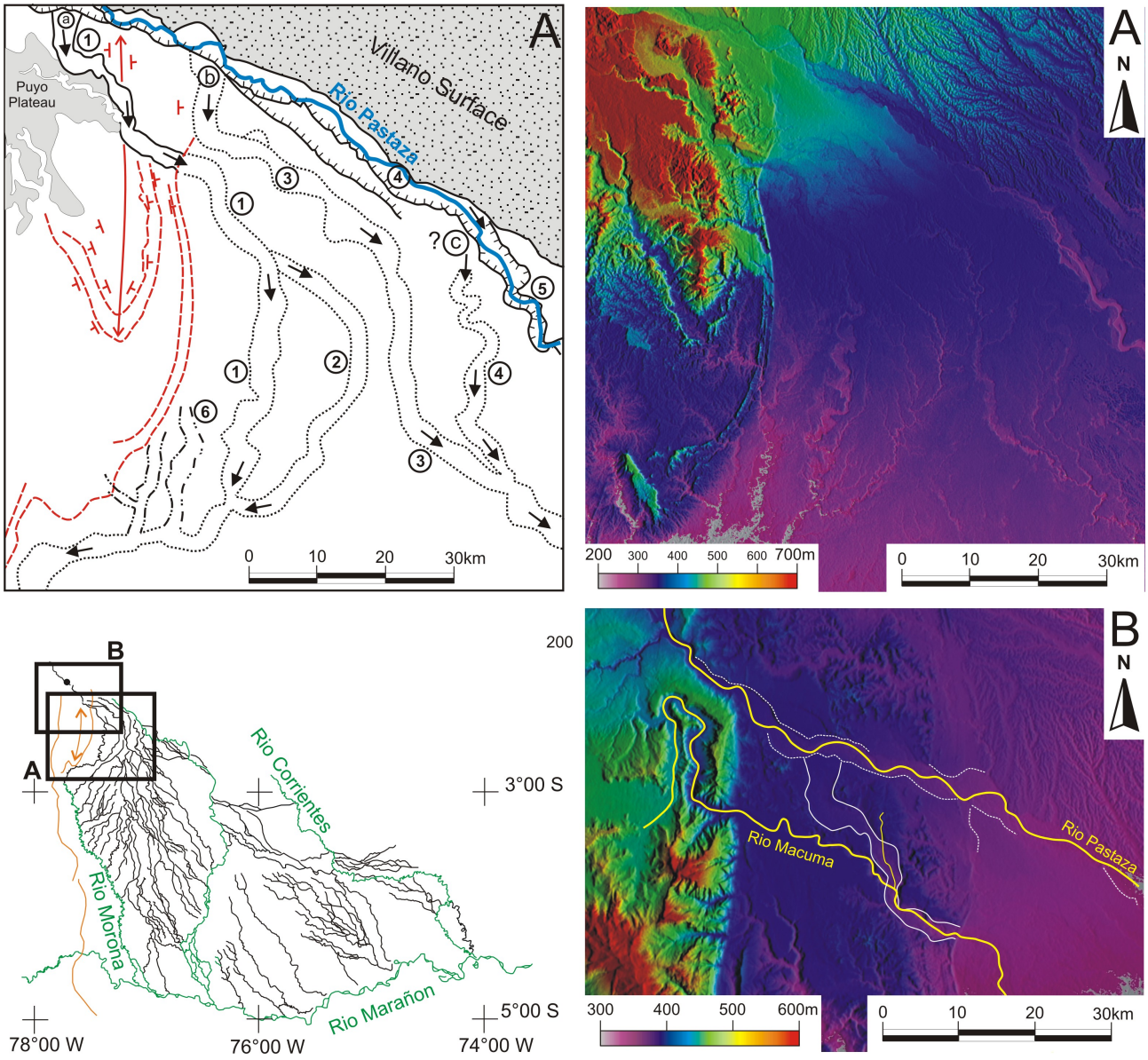

Figure 6 : To the left:map of the successive streams of the Rio Pastaza in the MCA. Those streams are bounded by pointed lines. The dashed-double pointed lines correspond to superimposed streams. Ticked lines indicate terrace scarps, Successive streams of the Rio Pastaza are numbered following chronology. Stream #5 is the modern Rio Pastaza. To the right: DEM SRTM V3. On the left bank of the Rio Pastaza the characteristic dendritic drainage network developed on top of the Villano surface. Some parts of this surface are also preserved on the right bank. At the bottom: topographic profile across the Pastaza Megafan and the Villano surface, we can quote the strongly dissected aspect of the Villano surface.

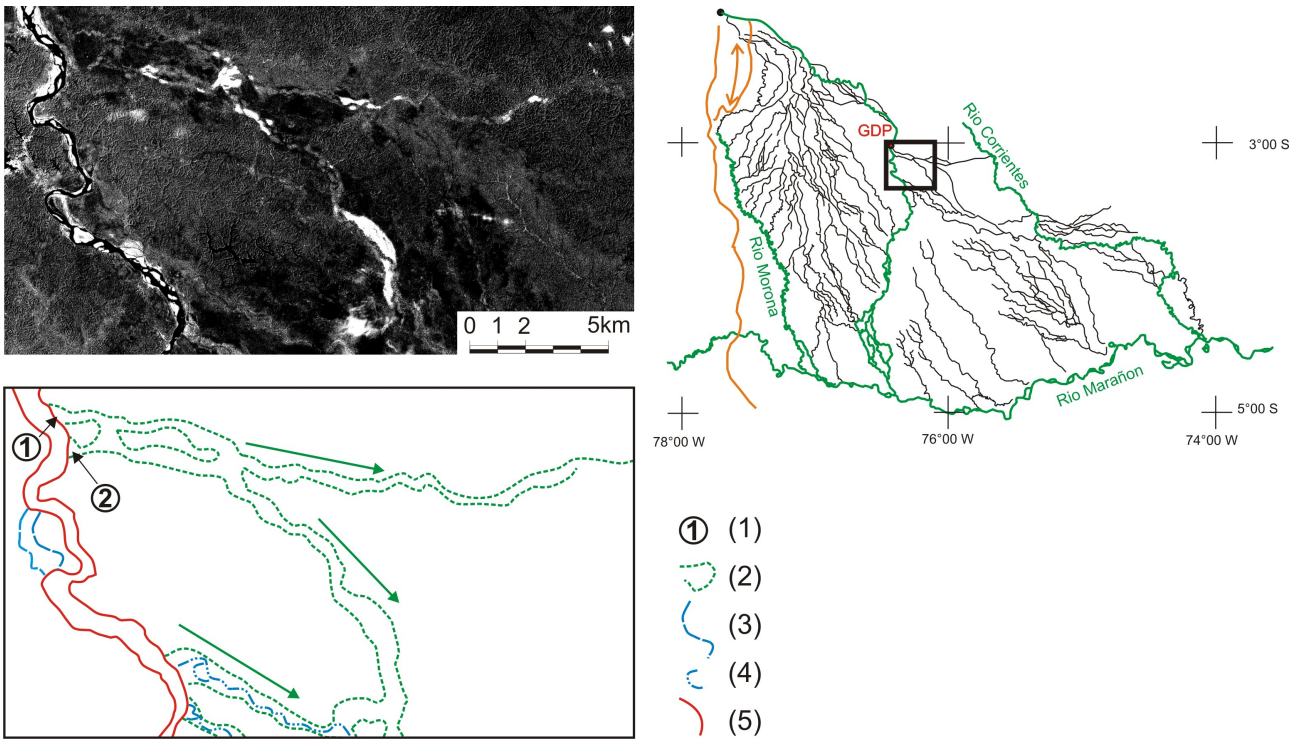

Figure 7: Satellite Image and interpretative map of the Great Diversion of the Pastaza are. Observe the sharp contrast between alluvial ridges (even abandoned and the floodplain area. 1) points of avulsion, 2) abandoned alluvial ridges, 3) abandoned loop of the Rio Pastaza, 4) underfitted streams re-occupying abandoned reaches, 5) modern Rio Pastaza Channel.

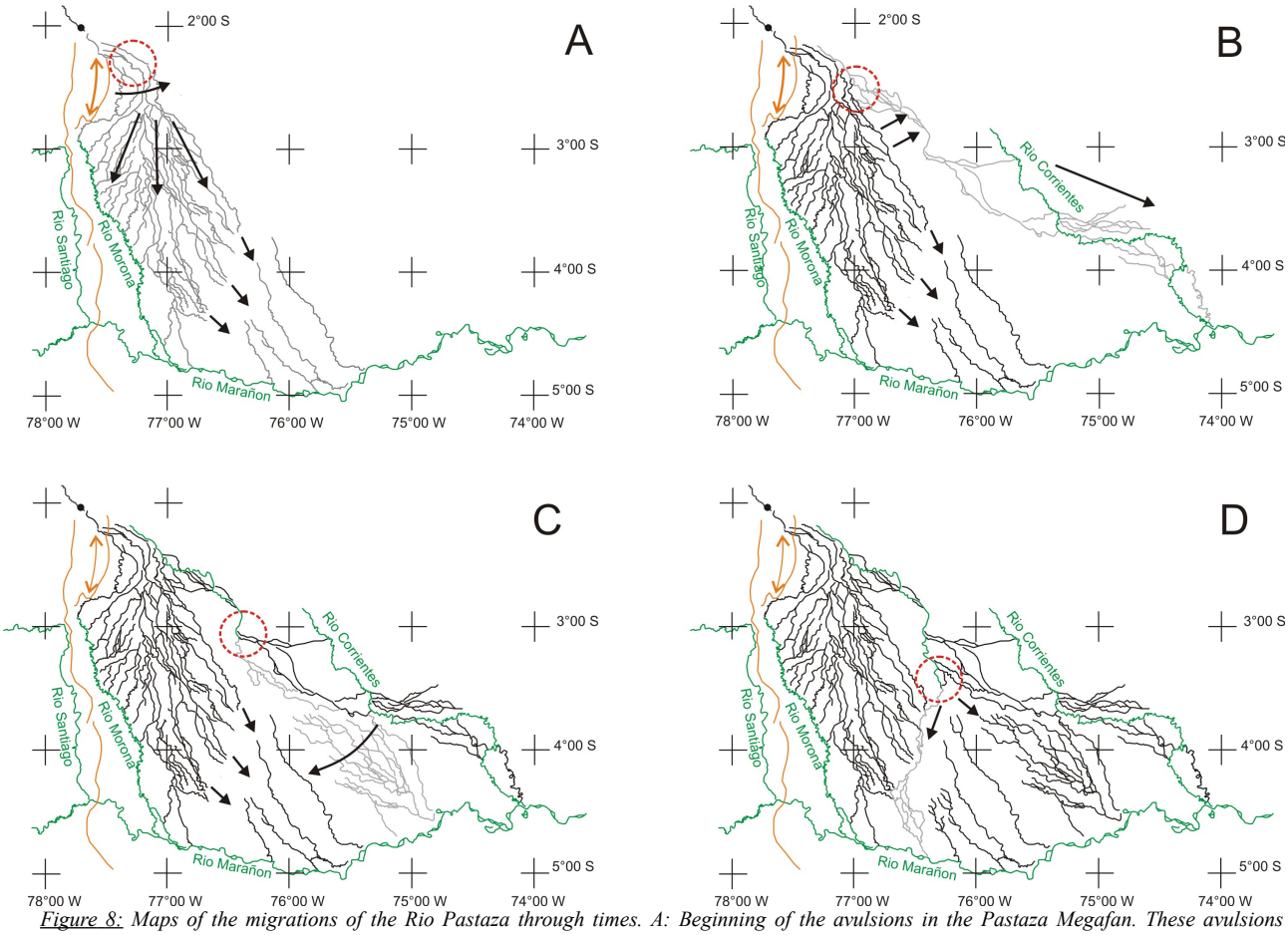

Figure 8: Maps of the migrations of the Rio Pastaza through times. A: Beginning of the avulsions in the Pastaza Megafan. These avulsions occurred after 21160 ± 260 yrs Cal BP, B: Great Diversion of the Rio Pastaza to the TCA. C: Avulsions in the TCA, this area was active around 9198±200 yrs Cal BP ou 8476 +/112 yrs Cal BP, D: Modern morphology of the drainage network resulting form the southward avulsion of the Rio Pastaza and the abandonment of the Rio Tigre/Corrientes area. This configuration is dated after 9198±200 yrs Cal BP or 8476 ±112 yrs Cal BP (see text for further explanations).

Satellite	Landsat			
years	1990		2000	
mosaics	S-18-00	S-18-05	S-18-00 2000	S18-05- 2000
# of landsat images	40	38	30	28
UTM Zone	18	18	18	18
Upper Latitude	0°	5° South	0°	5° South
period	1986/03/23 to 1994/06/30	1986/06/22 to 1994/07/14	1999/07/11 to 2001/10/02	1999/07/11 to 2001/09/20
Spatial resolution	28.5m	28.5m	14,25m	14.25m
Spectral band used	(TM7, TM4, TM2)+TM8		TM7, TM4, TM2	
Datum	WGS 84			

Table 1 : MrSID Image database used for the studied area with their characteristics.

Scenario		Time interval	Interval duration (years)			All Avulsions	Recurrence (years)		Most reliable	Recurrence of most reliable (years)	
1	Avulsions since 17920 years BP and 1691 AD	Between 17920 ± 70 BP and 1691 AD (Bes de Berc et al. 2005; Fritz in Gomez 1994)	(21,162 ± 261)—(1950–1691)	21,164(1)		108	195		88	240	
				20,903	20,903 ± 261	108	193	193 ± 2	88	237	237 ± 3
				20,642(2)		108	191		88	234	
2	Avulsions between 17920 and 8180 years BP	Between 17920 ± 70 BP and 8180 ± 120 BP (Bes de Berc et al. 2005; Räsänen et al. 1992)	(21,162 ± 261)—(9198 ± 200)	12,425(1)		84	148		67	185	
				11,964	11,964 +/461	84	142	142 ± 6	67	179	179 ± 7
				11,503(2)		84	137		67	172	
3	Avulsions between 17920 and 7650 years BP	Between 17920 ± 70 BP and 7658 ± 120 BP (Bes de Berc et al. 2005; Räsänen et al. 1992)	(21,162 ± 261)—(8476 ± 112)	13,059(1)		84	155		67	195	
				12,686	12,686 ± 373	84	151	151 ± 4	67	189	189 ± 6
				12,313(2)		84	147		67	184	
4	Avulsions between 8180 years BP and 1691 AD	Between 8180 ± 120 BP and 1691 AD (Räsänen et al. 1992; Fritz in Gomez 1994)	(9,198 ± 200)—(1950–1691)	9,139(1)		24	381		21	435	
				8,939	8,939 ± 200	24	372	372 ± 9	21	426	426 ± 10
				8,739(2)		24	364		21	416	
5	Avulsions between 7650 years BP and 1691 AD	Between 7658 ± 120 BP and 1691 AD (Räsänen et al. 1992; Fritz in Gomez 1994)	(8,476 ± 112)—(1950–1691)	8,329(1)		24	347		21	397	
				8,217	8,217 ± 112	24	342	342 ± 5	21	391	391 ± 6
				8,105(2)		24	338		21	386	

Table 2: Ages, conversions 14C ages/Calendar ages and computing of avulsions recurrence of the Rio Pastaza. Conversions 14C ages/Calendar ages were done following the INTCAL04 (Reimer et al., 2004). Columns "All avulsions" and "Global recurrence" take in account all the avulsions sites identified in the area (see Figure 4) while columns "Most reliable" and "Recurrence of most reliable" do not take in account the "supposed sites of avulsion" of Figure 2. (1) upper limit value, (2) lower limit value.

	Rio Pastaza Megafan			Rhine-Meuse delta		Saskatchewan	Kosi Megafan	Taquari Megafan	Brahmaputra river
	This study			Stouthamer and Berendsen (2000, 2001)		Morozova and Smith (1999, 2000)	Gole and Chitale (1966)	Assine (2005)	Bristow (1999)
Avulsions	108(1)	84(2)	24(3)	27(4)	87(4)	9	12	3	7
Interval (years)	~21,000	~12,300	~8,500	3,875	6,370	5,400	246 (1731–1977)	30 (1973–2003)	202 (1776–1978)
Recurrence (years)	~195	~145	~354	143	73	600	20.5	10	29
Average frequency (years)	0.51/100	0.68/100	0.28/100	0.7/100	1.4/100(4)	0.17/100	4.88/100	10/100	3.47/100

Table 3: Comparison of morphological parameters between the Pastaza Megafan and its catchment and other megafans. (1) Water discharge computed following the formula $Q = ka.A^{\alpha}$ with Q : discharge in $m.s^{-3}$, A : surface of the drainage basin in km^2, ka = 0.049 et α= 0.96 (Talling and Sowter 1998). (2) Streampower by length unit $\Omega=\gamma.Q.s$, with γ, specific weight of water (9810 $N.m^{-3}$), Q: discharge in $m.s^{-3}$, local slope in $m.m^{-1}$. (3) et (4) : (Bes de Berc et al. 2005). (5), after (Horton and DeCelles 2001). (6), after (Lavé and Avouac 2001). (7) after (Singh et al. 1993). (8) incision values of (Lavé and Avouac 2001) corresponding to the Main Boundary Thrust area for the Arun and Sun Kosi rivers, close to the Apex of the Kosi megafan.

	Catchment surface (km^2)	Fan surface (km^2)	Fan/catchment ratio	Discharge ($m\ s^{-3}$)(1)	Streampower ($W\ m^{-1}$)(2)	Incision values ($mm\ year^{-1}$)
Rio Pastaza	13,700	51,400	3.75	458	2.64×10^4	4.3(4)
MPA	13,700	13,750	1	458	2.64×10^4	4.3(4)
Rio Grande, Bolivia	~ 70,000(5)	~12,600(5)	0.18	2,195	5.10×10^4	n/a
Rio Pilcamayo	81,300(5)	~22,600(5)	0.28	2,534	2.76×10^4	n/a
Rio Parapeti	~ 8,000(5)	~5,800(5)	0.72	273	2.73×10^2	n/a
Kosi River	51,370(6)	~10,000(7)	0.19	1,631	5.12×10^4	1.5–2.5(8)

Table 4: Comparison of avulsion recurrence data between the Rio Pastaza megafan and other fluvial systems known for their frequent avulsions: the Rhine-Meuse delta (Stouthamer and Berendsen 2000) ; (Stouthamer and Berendsen 2001) ; the Saskatchewan river (Morozova and Smith 1999; Morozova and Smith 2000), the Kosi river megafan (Gole and Chitale 1966) and the Rio Taquari megafan (Assine 2005). (1) scenario 1 in table 2, (2) scenario 2 and 3 in Table 2, (3) scenario 4 and 5 in Table 2, (4) tectonically triggered avulsions that occurred between 5500 and 1625 BP (Stouthamer and Berendsen 2000), (5) avulsions which occurred between 7395 and 1000 BP (Stouthamer and Berendsen 2000), (6) between 1731 and 1977 (Gole and Chitale 1966; Wells and Dorr 1987).